

# Off-the-grid Recovery of Time and Frequency Shifts with Multiple Measurement Vectors

Maral Safari, Sajad Daei, Farzan Haddadi

**Abstract**—We address the problem of estimating time and frequency shifts of a known waveform in the presence of multiple measurement vectors (MMVs). This problem naturally arises in radar imaging and wireless communications. Specifically, a signal ensemble is observed, where each signal of the ensemble is formed by a superposition of a small number of scaled, time-delayed, and frequency shifted versions of a known waveform sharing the same continuous-valued time and frequency components. The goal is to recover the continuous-valued time-frequency pairs from a small number of observations. In this work, we propose a semidefinite programming which exactly recovers  $s$  pairs of time-frequency shifts from  $L$  regularly spaced samples per measurement vector under a minimum separation condition between the time-frequency shifts. Moreover, we prove that the number  $s$  of time-frequency shifts scales linearly with the number  $L$  of samples up to a log-factor. Extensive numerical results are also provided to validate the effectiveness of the proposed method over the single measurement vectors (SMVs) problem. In particular, we find that our approach leads to a relaxed minimum separation condition and reduced number of required samples.

**Index Terms**—Atomic norm minimization, super-resolution, multiple measurement vectors.

## I. INTRODUCTION

Over the past few years, there has been a growing interest in using super-resolution, a tool for recovering the high-resolution information from low-pass data. This technique is shown to be useful in many applications such as radar imaging [1], astronomy [2], communication systems [3], geophysics [4], microscopy [5] and also in the direction of arrival (DOA) estimation [6], [7] in which the aim is to estimate the directions of narrow-band sources by an array of sensors.

In this work, we study the problem of using an antenna array to estimate the time delays and Doppler (frequency) shifts of a known waveform. This problem naturally occurs in active radar imaging [8], [9] and multi-path channel identification in wireless communications [9]. More precisely, in these applications, a known waveform  $x(t)$  is transmitted and reflections from moving sources are received at the  $R$ -element antenna array. Writing in mathematical terms, we observe a signal ensemble

$$y_m(t) = \sum_{j=1}^s b_{jm} x(t - \bar{\tau}_j) e^{i2\pi \bar{\nu}_j t}, \quad m = 1, \dots, R, \quad (1)$$

at the array where  $R$  is the number of array elements,  $b_{jm}$  is the attenuation factor corresponding to the time-Doppler shifts  $(\bar{\tau}_j, \bar{\nu}_j)$ , and  $s$  is the number of moving sources. In active radar imaging, estimating delay and Doppler shifts provides

valuable information about the location and relative velocity of the targets in the scene. Besides, in wireless communications [9], model (1) represents a scenario where a mobile user is rapidly moving and sends a known training sequence to a base station (BS) for channel estimation and equalization purposes. In case that the communication channel is frequency selective, the signal arrives at the BS with multiple different delays and Doppler shifts. Estimating the delays and Doppler shifts is necessary for BS in order to remove the inter-symbol interference.

By taking regularly spaced samples of  $y(t)$  in model (1) (see Section (II) for a detailed description), we have a measurement vector at each antenna composed of  $L$  samples. Considering a  $R$ -element antenna array, we encounter multiple measurement vectors (MMVs) by assuming that the delay-Doppler pairs remain fixed at the output of array. It is worth mentioning that the aforementioned method for accessing MMVs is different from what has been considered in the literature (see for example [10], [11]), since, there, MMVs refer to multiple snapshots in the time domain. However, here we assume  $R$  measurements are observed via an  $R$ -element antenna array. It is also possible to have multiple measurements in time (alternatively meant to be multiple snapshots) by choosing the probing signal  $x(t)$  to be periodic<sup>1</sup>. There are, however, a few constraints imposed by practical scenarios: The probing signal  $x(t)$  has finite bandwidth  $B$ , the received signals at the array are only observed during a finite interval of length  $T$ , the delay-Doppler pairs has finite support, i.e.  $(\bar{\tau}_j, \bar{\nu}_j) \in [-\frac{T}{2}, \frac{T}{2}] \times [-\frac{B}{2}, \frac{B}{2}]$ . By the latter assumptions, and since the effective support of the probing signal in the time and frequency domain must be greater than the delay-Doppler shifts,  $x(t)$  and  $y(t)$  must be both approximately time- and band-limited. Hence, the natural resolution limit, i.e. the accuracy up to which  $(\bar{\tau}_j, \bar{\nu}_j)$  can be uniquely resolved, is  $\frac{1}{B}$  and  $\frac{1}{T}$  in the delay and Doppler directions, respectively. This resolution limit can be achieved by using a standard digital matched filter in order to identify the delay-Doppler pairs. In this paper, we show that this resolution limit can be broken by assuming that the delay-Doppler pair  $(\bar{\tau}_j, \bar{\nu}_j)$  can take any continuous values in  $[-\frac{T}{2}, \frac{T}{2}] \times [-\frac{B}{2}, \frac{B}{2}]$  and is not constrained to be on a predefined domain of grids which is the case in the well-known theory of compressed sensing (CS) [12]. Specifically, using the on-grid assumption in CS,  $\ell_{1,2}$  minimization can be applied to recover the unknowns  $(\bar{\tau}_j, \bar{\nu}_j)$  from MMVs. However, most CS-based methods<sup>2</sup> including  $\ell_{1,2}$  minimization needs

M. Safari, S. Daei and F. Haddadi are with the School of Electrical Engineering, Iran University of Science & Technology.

<sup>1</sup>See [9, Appendix H] for a detailed discussion.

<sup>2</sup>See e.g. [13], [14].

incoherence property which does not generally hold when the grids are fine and hence we encounter an unavoidable basis mismatch between on-the-grid and true delay-Doppler pairs. Our goal in this paper is to estimate the continuous delay-Doppler pairs  $(\bar{\tau}_j, \bar{\nu}_j)$ ,  $j = 1, \dots, s$  from these MMVs. To achieve this goal, we propose general atomic norm problems (inspired by [15]) for two-dimensional (2D) super-resolution in the noise-free and noisy cases equipped with MMVs. To the best of the authors' knowledge, super-resolving 2D continuous parameters from MMVs using the concepts of atomic norm minimization has not been addressed before and indeed most of the prior works can be seen as a special case of it. Further, our proposed problems can be viewed as a continuous counterpart of  $\ell_{1,2}$  minimization in CS. However, unlike  $\ell_{1,2}$  which is designed for recovering one on-grid parameter, our framework, instead, is seeking to recover two continuous off-grid unknowns (i.e. delay-Doppler pairs). We show that our proposed atomic norm problems can be efficiently solved using semidefinite programming and the continuous delay-Doppler shifts<sup>3</sup> can be exactly recovered. Moreover, we theoretically prove that if we take  $L$  noise-free samples per measurement vector, up to  $\mathcal{O}(\frac{L}{\log(L^6 T)})$  delay-Doppler pairs can be exactly recovered with high probability using our proposed method provided that a certain minimum separation condition between the time-frequency shifts is satisfied. Numerical results also demonstrate that our proposed approach leads to improved (relaxed) minimum separation condition compared to the case of single measurement vector (SMV) problem proposed in [9] in both noise-free and noisy cases. Besides, we show that under a fixed minimum separation between the delay-Doppler pairs, the number of required samples for successful and robust recovery decreases.

#### A. Related Works and Key Differences

Conventional subspace-based methods such as MUSIC and ESPRIT [16], [17], assume that the signal amplitudes  $b_{jm}$  are uncorrelated and the covariance matrix corresponding to samples of each array element is low-rank. The performance of these approaches are prone to be corrupted against noise and correlations between sources  $b_{jm}$ .

The theory of super-resolution using convex optimization is first initiated by Candes et al. in [18]. They propose a problem for recovering off-grid time-domain spikes from low-pass Fourier measurements in the SMV case. They show that the continuous spikes in the time domain can be exactly recovered by solving semidefinite programming provided that a minimum separation between sources is satisfied.

Tang et al. in [19] study super-resolution problem in the framework of CS. They propose an atomic norm minimization where the frequency spikes of a signal are recovered from its partial time-domain samples. Their work can be regarded as the continuous counterpart of  $\ell_1$  minimization in CS. The difference with [18] lies in the fact that they consider only partial random observations rather than full observations in [18].

<sup>3</sup>Throughout, we occasionally use time-frequency shifts instead of delay-Doppler shifts.

Hyder et al. propose a non-convex algorithm based on smoothed  $\ell_{0,2}$ <sup>4</sup> to extract the joint (common) sparsity pattern of 1D signals from MMVs. They investigate both narrow-band and broad-band DOA estimation and show that using MMVs allows a larger sensor spacing than the smallest half-wavelength of the signal in case of broad-band signal. Unlike the subspace-based methods, this method does not require the number of 1D sources in advance. However, the DOAs are assumed on-the-grid which somewhat limits the applicability of the method. Moreover, an issue associated with this non-convex approach is that its stability against measurement noise is not assured.

Yang et al. in [11] study recovering signals which share the same 1D frequency parameter from MMVs. They propose an atomic norm framework to solve this problem and study the advantage of using MMVs over SMV. They show that the availability of MMVs results in relaxed minimum separation condition and reduced number of required measurements. The observed signal is scaled samples of the sum of  $s$  sinusoids and coincides with model (1) when the delays are ignored or alternatively when we have only frequency shifts. However, most of the proof techniques in [11] can not be applied to model (1). In particular, our atomic framework and choice of atoms (which turns to be a multiplication of two Dirichlet kernel) are completely different from that in [11], since model (1) deals with two unknown parameters in two different domains (i.e. time and frequency shifts). In fact, 1D methods (e.g. in [17], [18]) can not be used for proofs in 2D case.

Li et al. in [10] investigate the benefit of incorporating MMVs into off-the-grid frequency estimation and denoising. They develop an atomic norm minimization that aims to estimate and denoise spectrally sparse signals from partial noisy MMVs. They provide numerical experiments showing the performance gain of their method over SMV when the number of measurement vectors increases. They obtain a performance guaranty to denoise MMV signals which share common 1D frequency components. Their analysis and proofs extend the results of [19] for MMV signals for 1D frequency estimation. Again, their proof approach fails to apply for estimating 2D time-frequency shifts.

Heckel et al. in [9] tackle the problem of identifying time-frequency shifts in radar scenario. The observed signal at receiver is a scaled superposition of time and frequency shifted versions of a known waveform. Thus, their model can be regarded as a special case of our model (1) where only one element is used at the array. Specifically, an atomic norm approach is provided to recover the continuous delay-Doppler pairs using SMV. As opposed to what is done in [9], we benefit from the common atomic sparsity pattern of MMVs at the outputs of the sensor array. Our work can be viewed as an extension of the SMV work [9] to the MMV case. However, this nontrivial generalization comes with major mathematical differences, of which we can mention the uniqueness proof of our proposed atomic problem that deals with vector-valued dual polynomials which is much more challenging than the scalar-valued polynomial used in [9].

<sup>4</sup>A function that promotes the number of blocks with non-zero  $\ell_2$  norm.

There also exist other works that might be somehow relevant to our work such as [20] which deals with recovering three continuous parameters in multiple input multiple output (MIMO) scenario. However, besides the fact that their model is different from ours, their work does not use the availability of MMVs.

### B. Outline and Notations

Throughout the paper, scalars are denoted by lowercase letters, vectors by lowercase boldface letters, and matrices by uppercase boldface letters. The  $k$ th element of a vector  $\mathbf{x}$  is denoted by  $x(k)$ . The absolute value of a scalar, the element-wise absolute value of a vector and the cardinality of a set are shown by  $|\cdot|$ . The infinity norm is  $\|\mathbf{z}\|_\infty = \max_k |z_k|$ . In addition,  $\|\cdot\|_1$ ,  $\|\cdot\|_2$  and  $\|\cdot\|_F$  are reserved for  $\ell_1$ ,  $\ell_2$  and Frobenius norms, respectively. We define  $\|\mathbf{A}\| := \max_{\|\mathbf{v}\|_2=1} \|\mathbf{A}\mathbf{v}\|_2$  and  $\|\mathbf{A}\|_{2,\infty} := \max_j \|\mathbf{a}_j\|_2$ , where  $\mathbf{a}_j$  denotes the  $j$ -th row of a matrix  $\mathbf{A}$ . The operator  $\langle \cdot, \cdot \rangle_{\mathbb{R}}$  stands for the real part of the inner product of two vectors. We use a 2D index for vectors or matrices. Indeed, by  $[\mathbf{z}]_{(k,l)}$ ,  $k, l = -N, \dots, N$ , we mean that  $\mathbf{z} = [z(-N, -N), z(-N, -N+1), \dots, z(-N, N), z(-N+1, -N), \dots, z(N, N)]$ . The operators  $\text{tr}(\cdot)$  and  $(\cdot)^H$  represent the trace and Hermitian of a matrix, respectively.  $x^*$  is the conjugate of  $x$ . To show that  $\mathbf{A}$  is a positive semidefinite matrix, we write  $\mathbf{A} \geq 0$ .  $\mathbb{E}[\cdot]$  and  $\mathbb{P}[\cdot]$  denote the expectation and probability of an event, respectively.  $\mathbb{S}^{R-1} = \{\boldsymbol{\varphi} \in \mathbb{C}^{R \times 1} : \|\boldsymbol{\varphi}\|_2 = 1\}$  denote the unit complex or real sphere. Finally, we use numerical constants  $c, \tilde{c}, c', c_1, c_2, \dots$  which take on different values at different places.

## II. SYSTEM MODEL AND RECOVERY VIA CONVEX OPTIMIZATION

As we assumed earlier,  $(\bar{\tau}_j, \bar{\nu}_j) \in [-\frac{T}{2}, \frac{T}{2}] \times [\frac{B}{2}, \frac{B}{2}]$ . Based on 2BT-Theorem [21], [22], we can take samples of  $y_m(t)$  in the interval  $[-\frac{T}{2}, \frac{T}{2}]$  at rate  $\frac{1}{B}$ . So, we totally have  $L := BT$  samples<sup>5</sup> of the form (see Appendix A for a detailed derivation):

$$y_{pm} = \sum_{j=1}^s b_{jm} \sum_{k,l=-N}^N D_N(\frac{l}{L} - \tau_j) D_N(\frac{k}{L} - \nu_j) x_{p-l} e^{i2\pi(\frac{kp}{L})}$$

$$p = -N, \dots, N \quad L = 2N + 1, \quad m = 1, \dots, R, \quad (2)$$

where

$$D_N(t) := \frac{1}{L} \sum_{k=-N}^N e^{i2\pi tk} \quad (3)$$

is the Dirichlet kernel.  $\tau_j := \frac{\bar{\tau}_j}{T}$  and  $\nu_j := \frac{\bar{\nu}_j}{B}$  are the normalized time-frequency shifts, respectively.  $x_l$  is the  $l$ -th sample of the probing signal  $x(t)$  and is assumed to be  $L$ -periodic. It is easy to verify that  $(\tau_j, \nu_j) \in [-\frac{1}{2}, \frac{1}{2}]^2$ . Due to the periodicity property, without loss of generality, we assume that  $(\tau_j, \nu_j) \in [0, 1]^2$ . Define atoms  $\mathbf{a} \in \mathbb{C}^{L^2 \times 1}$  with elements

$$[\mathbf{a}(\mathbf{r})]_{(k,l)} = D_N(\frac{l}{L} - \tau) D_N(\frac{k}{L} - \nu), \quad \mathbf{r} = [\tau, \nu]^T, \quad (4)$$

$$k, l = -N, \dots, N.$$

<sup>5</sup>Without loss of generality, we assume that  $L$  is an odd integer.

By using the definition of Dirichlet kernel in (3), the atoms  $\mathbf{a} \in \mathbb{C}^{L^2 \times 1}$  can also be reformulated as

$$\mathbf{a}(\mathbf{r}) = \mathbf{F}^H \mathbf{f}(\mathbf{r}), \quad (5)$$

where  $[\mathbf{f}(\mathbf{r})]_{(m,n)} := e^{-i2\pi(m\tau+n\nu)}$ , and  $\mathbf{F}^H$  is the inverse 2D discrete Fourier transform whose entries are given by

$$[\mathbf{F}^H]_{(k,l),(m,n)} := \frac{1}{L^2} e^{i2\pi(\frac{mk+nl}{L})}. \quad (6)$$

The relation (2) can be reformulated in matrix form as

$$\mathbf{Y} = \mathbf{G}\mathbf{X} \in \mathbb{C}^{L \times R}, \quad (7)$$

where

$$\mathbf{X} = \sum_{j=1}^s \mathbf{a}(\mathbf{r}_j) \mathbf{b}_j^H = \sum_{j=1}^s c_j \mathbf{a}(\mathbf{r}_j, \boldsymbol{\varphi}_j) = \sum_{j=1}^s c_j \mathbf{a}(\mathbf{r}_j) \boldsymbol{\varphi}_j^H,$$

$$\mathbf{r}_j := [\tau_j, \nu_j]^T, \quad (8)$$

$\mathbf{b}_j^H = [b_{j1}, \dots, b_{jR}] \in \mathbb{C}^{1 \times R}$  is the attenuation vector,  $c_j = \|\mathbf{b}_j\|_2 > 0$ , and  $\boldsymbol{\varphi}_j = c_j^{-1} \mathbf{b}_j \in \mathbb{S}^{R-1}$ . Here,  $\mathbf{G} \in \mathbb{C}^{L \times L^2}$  is the Gabor matrix whose elements are given by

$$[\mathbf{G}]_{p,(k,l)} := x_{p-l} e^{i2\pi(\frac{kp}{L})}, \quad k, l, p = -N, \dots, N. \quad (9)$$

We observe from (8) that  $\mathbf{X} \in \mathbb{C}^{L^2 \times R}$  is a sparse combination of a few matrix atoms  $\mathbf{a}(\mathbf{r}_j, \boldsymbol{\varphi}_j)$ ,  $j = 1, \dots, s$  belonging to the atomic set

$$\mathcal{A} := \{\mathbf{a}(\mathbf{r}, \boldsymbol{\varphi}) := \mathbf{a}(\mathbf{r}) \boldsymbol{\varphi}^H : \mathbf{r} \in [0, 1]^2, \quad \boldsymbol{\varphi} \in \mathbb{S}^{R-1}\}.$$

Hence, to extract  $\mathbf{X} \in \mathbb{C}^{L^2 \times R}$  from the underdetermined observations  $\mathbf{Y} \in \mathbb{C}^{L \times R}$ , inspired by [15], we propose the atomic norm minimization

$$\min_{\mathbf{Z} \in \mathbb{C}^{L^2 \times R}} \|\mathbf{Z}\|_{\mathcal{A}} \quad \text{subject to } \mathbf{Y} = \mathbf{G}\mathbf{Z}, \quad (10)$$

where the atomic norm  $\|\mathbf{X}\|_{\mathcal{A}}$  is defined as

$$\|\mathbf{X}\|_{\mathcal{A}} := \inf\{t > 0 : \mathbf{X} \in t \text{conv}(\mathcal{A})\} =$$

$$\inf\left\{\sum_j c_j : \mathbf{X} = \sum_j c_j \mathbf{a}(\mathbf{r}_j, \boldsymbol{\varphi}_j), c_j > 0, \mathbf{r}_j \in [0, 1]^2\right\}, \quad (11)$$

and  $\text{conv}(\mathcal{A})$  denotes the convex hull of  $\mathcal{A}$ .

## III. MAIN RESULT

In the following, we state our main result which provides conditions for exact recovery of  $\mathbf{X}$  in (10).

**Theorem 1.** Suppose that the entries of the probing signal  $x_l$ ,  $l = -N, \dots, N$ , are i.i.d. random variables distributed as  $\mathcal{N}(0, \frac{1}{L})$  where  $L = 2N + 1$ . Let  $\mathbf{Y} \in \mathbb{C}^{L \times R}$  be the observed matrix at the  $R$ -element antenna array as in (7) i.e.

$$\mathbf{Y} = \mathbf{G}\mathbf{X} \in \mathbb{C}^{L \times R}, \quad \mathbf{X} = \sum_{\mathbf{r}_j \in \mathcal{S}} c_j \mathbf{a}(\mathbf{r}_j, \boldsymbol{\varphi}_j) \quad (12)$$

with  $L > 1024$ . Here,  $\mathbf{G}$  is the Gabor matrix defined in (9) and  $\mathcal{S}$  is the location of delay-Doppler pairs corresponding to  $\mathbf{X}$ . Fix  $\delta > 0$ . Assume that  $\boldsymbol{\varphi}_j$ ,  $j = 1, \dots, s$  are independent and uniformly distributed on the unit sphere  $\mathbb{S}^{R-1}$  with  $\mathbb{E}[\boldsymbol{\varphi}_j] = 0$

and that the set of time-frequency shifts  $\mathcal{S} = \{\mathbf{r}_1, \mathbf{r}_2, \dots, \mathbf{r}_s\} \subset [0, 1]^2$  obeys the minimum separation condition

$$\max(|\tau_j - \tau_{j'}|, |\nu_j - \nu_{j'}|) \geq \frac{2.38}{N}, \quad (13)$$

$$\forall (\tau_j, \nu_j), (\tau_{j'}, \nu_{j'}) \in \mathcal{S} \quad \text{with } j \neq j'. \quad (14)$$

Moreover, assume that

$$s \leq c \frac{L}{\log^3(\frac{L^6 R}{\delta})} \quad (15)$$

where  $c$  is a constant. Then, with probability at least  $1 - \delta$ ,  $\mathbf{X}$  is the unique solution of (10).

Proof. See Appendix C.

The proof of Theorem 1 is built upon constructing a certain dual certificate for (10). In the following proposition, we describe the desired form of a valid vector-valued dual certificate which guaranties the optimality of  $\mathbf{X}$  in (10).

**Proposition 1.** Assume that  $\mathbf{Y} = \mathbf{G}\mathbf{X}$  with  $\mathbf{X} = \sum_{\mathbf{r}_j \in \mathcal{S}} c_j \mathbf{a}(\mathbf{r}_j, \varphi_j)$  where  $\mathcal{S}$  is the location of delay-Doppler pairs corresponding to  $\mathbf{X}$ . If there exists a vector-valued dual polynomial  $\mathbf{q} : [0, 1]^2 \rightarrow \mathbb{C}^{R \times 1}$ ,

$$\mathbf{q}(\mathbf{r}) = \mathbf{\Lambda}^H \mathbf{G} \mathbf{a}(\mathbf{r}) \quad (16)$$

satisfying

$$\begin{aligned} \mathbf{q}(\mathbf{r}_j) &= \varphi_j, & \mathbf{r}_j &\in \mathcal{S}, \\ \|\mathbf{q}(\mathbf{r})\|_2 &\leq 1, & \mathbf{r} &\in [0, 1]^2 \setminus \mathcal{S}, \end{aligned} \quad (17)$$

then  $\mathbf{X}$  is the optimal solution of (10).

The problem (10) involves finding infinitely many variables and can not be directly solved. To practically solve (10), we first obtain its dual formulation obtained from a standard Lagrangian approach (e.g. see [23, Chapter 6]):

$$\max_{\mathbf{\Lambda} \in \mathbb{C}^{L \times R}} \text{Re} \langle \mathbf{\Lambda}, \mathbf{Y} \rangle_F \quad \text{subject to } \|\mathbf{G}^H \mathbf{\Lambda}\|_{\mathcal{A}}^d \leq 1, \quad (18)$$

where  $\mathbf{\Lambda} = [\mathbf{\Lambda}_{pm}] \in \mathbb{C}^{L \times R}$ ,  $m = 1, \dots, R$ ,  $p = -N, \dots, N$  and

$$\|\mathbf{V}\|_{\mathcal{A}}^d := \sup_{\|\mathbf{Z}\|_{\mathcal{A}} \leq 1} \text{Re} \langle \mathbf{V}, \mathbf{Z} \rangle \quad (19)$$

is the dual norm. Hence, using (5), we have

$$\begin{aligned} \|\mathbf{G}^H \mathbf{\Lambda}\|_{\mathcal{A}}^d &= \sup_{\substack{\|\varphi\|_2=1 \\ \mathbf{r} \in [0, 1]^2}} \langle \mathbf{G}^H \mathbf{\Lambda}, \mathbf{a}(\mathbf{r}) \varphi^H \rangle_F = \\ &= \sup_{\substack{\|\varphi\|_2=1 \\ \mathbf{r} \in [0, 1]^2}} \langle \varphi, (\mathbf{F} \mathbf{G}^H \mathbf{\Lambda})^H \mathbf{f}(\mathbf{r}) \rangle = \sup_{\mathbf{r} \in [0, 1]^2} \|(\mathbf{F} \mathbf{G}^H \mathbf{\Lambda})^H \mathbf{f}(\mathbf{r})\|_2, \end{aligned} \quad (20)$$

where we used Holder inequality in the last step. Hence, the constraint of (18) becomes equivalent to

$$\begin{aligned} \|(\mathbf{F} \mathbf{G}^H \mathbf{\Lambda})^H \mathbf{f}(\mathbf{r})\|_2^2 &= \sum_{m=1}^R \left| \sum_{k, l=-N}^N [\mathbf{F} \mathbf{G}^H \mathbf{\Lambda}]_{(k, l), m} e^{i2\pi(k\tau + l\nu)} \right|^2 \\ &\leq 1, \quad \forall \mathbf{r} \in [0, 1]^2. \end{aligned} \quad (21)$$

By replacing (21), the dual problem (18) involves infinitely many constraints. The following proposition which is an adaptation of [24, Proposition 2.4] and [25, Corollary 4.27] provides a tractable sufficient condition for the constraint (21).

**Proposition 2.** Let  $\mathbf{P} = [P_{(k, l), m}]$  be a matrix in  $\mathbb{C}^{L^2 \times R}$  with  $k, l = -N, \dots, N$ ,  $m = 1, \dots, R$ ,  $L = 2N + 1$ . If

$$\sum_{m=1}^R \left| \sum_{k, l=-N}^N P_{(k, l), m} e^{i2\pi(k\tau + l\nu)} \right|^2 \leq 1, \quad \forall \mathbf{r} \in [0, 1]^2,$$

then there exists a Hermitian positive semidefinite matrix  $\mathbf{Q} \in \mathbb{C}^{L^2 \times L^2}$  obeying

$$\begin{aligned} \begin{bmatrix} \mathbf{Q} & \mathbf{P} \\ \mathbf{P}^H & \mathbf{I}_R \end{bmatrix} &\geq 0, \quad \text{trace}((\mathbf{\Theta}_k \otimes \mathbf{\Theta}_l) \mathbf{Q}) = \delta_{(k, l)}, \\ \forall k, l &= -N, \dots, N, \end{aligned} \quad (22)$$

where

$$\delta_{(k, l)} := \begin{cases} 1, & (k, l) = (0, 0), \\ 0, & \text{o.w.} \end{cases}$$

is the indicator function and  $\mathbf{\Theta}_k$  stands for the Toeplitz matrix composed of ones on the  $k$ -th diagonal and zeros elsewhere.

By exploiting Proposition 2, the dual problem (18) is relaxed to the following semidefinite programming (SDP):

$$\begin{aligned} \max_{\substack{\mathbf{\Lambda} \in \mathbb{C}^{L \times R} \\ \mathbf{Q} \in \mathbb{C}^{L^2 \times L^2}, \mathbf{Q} \geq 0}} \quad & \text{Re} \langle \mathbf{\Lambda}, \mathbf{Y} \rangle_F \quad \text{subject to} \\ \begin{bmatrix} \mathbf{Q} & \mathbf{F} \mathbf{G}^H \mathbf{\Lambda} \\ \mathbf{\Lambda}^H \mathbf{G} \mathbf{F}^H & \mathbf{I}_R \end{bmatrix} &\geq 0, \quad \text{trace}((\mathbf{\Theta}_k \otimes \mathbf{\Theta}_l) \mathbf{Q}) = \delta_{(k, l)}, \\ \forall k, l &= -N, \dots, N, \end{aligned} \quad (23)$$

**Remark 1.** The problem (23) is only a relaxation for (18). In fact, the size of  $\mathbf{Q}$  could be larger than  $L^2 \times L^2$ , since the sum of squares expression of a bivariate positive trigonometric polynomial with degree  $(L, L)$  might have factors with degree greater than the minimum degree  $(L, L)$ . However, as simulation results of [9], [25] indicate, relaxations of minimal degree often lead to optimal solutions in practice<sup>6</sup>.

When the measurements are contaminated with noise, i.e.  $\mathbf{Y} = \mathbf{G}\mathbf{X} + \mathbf{W}$ , we solve the following problem:

$$\min_{\mathbf{Z}} \|\mathbf{Z}\|_{\mathcal{A}} \quad \text{subject to } \|\mathbf{Y} - \mathbf{G}\mathbf{Z}\|_F \leq \eta, \quad (24)$$

where  $\eta$  is an upper-bound on the standard deviation of noise. Moreover, the SDP problem in this case takes the form

$$\begin{aligned} \max_{\substack{\mathbf{\Lambda} \in \mathbb{C}^{L \times R} \\ \mathbf{Q} \in \mathbb{C}^{L^2 \times L^2}, \mathbf{Q} \geq 0}} \quad & \text{Re} \langle \mathbf{\Lambda}, \mathbf{Y} \rangle_F - \eta \|\mathbf{\Lambda}\|_F \quad \text{subject to} \\ \begin{bmatrix} \mathbf{Q} & \mathbf{F} \mathbf{G}^H \mathbf{\Lambda} \\ \mathbf{\Lambda}^H \mathbf{G} \mathbf{F}^H & \mathbf{I}_R \end{bmatrix} &\geq 0, \quad \text{tr}((\mathbf{\Theta}_k \otimes \mathbf{\Theta}_l) \mathbf{Q}) = \delta_{(k, l)}, \\ \forall k, l &= -N, \dots, N, \end{aligned} \quad (25)$$

Now, we are ready to state the procedure of finding delay-Doppler pairs from the dual solution in both noiseless and noisy cases. Write the vector-valued dual polynomial

$$\mathbf{q}(\mathbf{r}) = \hat{\mathbf{\Lambda}}^H \mathbf{G} \mathbf{a}(\mathbf{r}), \quad (26)$$

where  $\hat{\mathbf{\Lambda}}$  is the solutions of the SDP problems (23) and (25). Proposition 1 suggests that an estimate  $\hat{\mathcal{S}}$  of the set of delay-Doppler pairs  $\mathcal{S}$  can be obtained from

$$\hat{\mathcal{S}} = \{\mathbf{r} \in [0, 1]^2 \mid \|\mathbf{q}(\mathbf{r})\|_2 = 1\}. \quad (27)$$

<sup>6</sup>See [9, Section 6] and [25, Remark 3.6] for a detailed discussion.

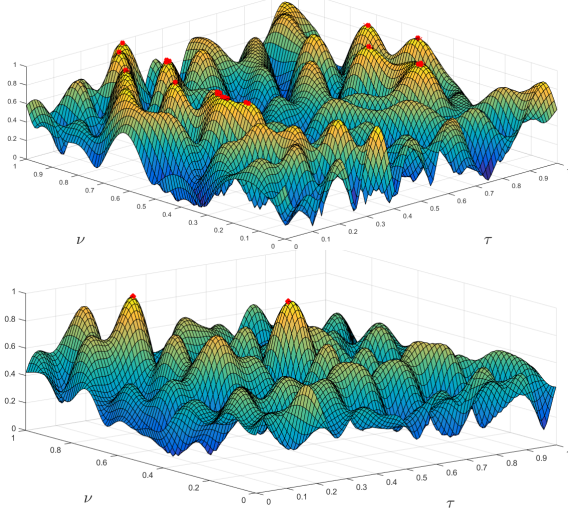


Fig. 1: Noiseless case. The true sources are located at  $\mathbf{r}_1 = (0.2, 0.5)$ ,  $\mathbf{r}_2 = (0.8, 0.5)$ . We set  $N = 4$  and solve (23). Top and bottom images show  $\|\mathbf{q}(\mathbf{r})\|_2$  for SMV ( $R = 1$ ) and MMV ( $R = 10$ ) cases, respectively. Red markers show where  $\|\mathbf{q}(\mathbf{r})\|_2$  equals one.

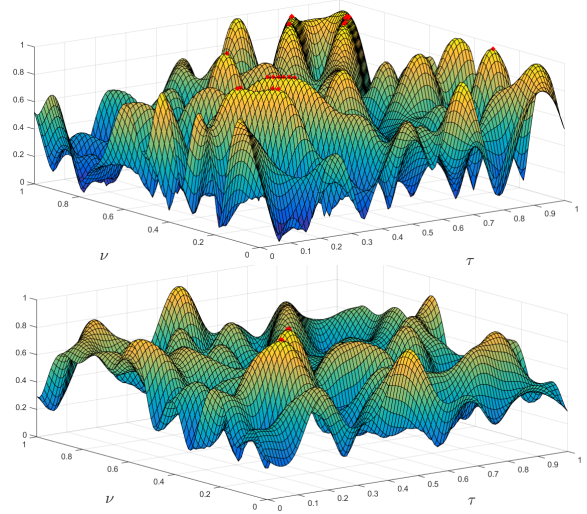


Fig. 2: Noiseless case. The true sources are located at  $\mathbf{r}_1 = (0.2, 0.2)$  and  $\mathbf{r}_2 = (0.3, 0.3)$ . We set  $N = 4$  and solve (23). Top and bottom images show  $\|\mathbf{q}(\mathbf{r})\|_2$  for SMV ( $R = 1$ ) and MMV ( $R = 30$ ) cases, respectively. Red markers show where  $\|\mathbf{q}(\mathbf{r})\|_2$  equals one.

#### IV. SIMULATION RESULTS

In this section, we consider the benefits of using MMVs in both noiseless and noisy cases. Let the probing signal  $x_l$ ,  $l = -N, \dots, N$  and the coefficients  $b_{jm}$  be drawn from i.i.d. uniform distribution on the complex unit sphere. Choose  $N = 4$ . First, in top and bottom of Figure 1, we consider two time-frequency shifts in locations  $\mathbf{r}_1 = (0.2, 0.5)$  and  $\mathbf{r}_2 = (0.8, 0.5)$  with  $R = 1$  and  $R = 10$ , respectively. We implement the problem (23) via SDPT3 in CVX package [26] and plot  $\|\mathbf{q}(\mathbf{r})\|_2$  where  $\mathbf{q}(\mathbf{r})$  is obtained from (26). Then, according to (27), we estimate time-frequency shifts by checking where  $\|\mathbf{q}(\mathbf{r})\|_2$  achieves one. As it turns out from top and bottom images of Figure 1, while the SMV case ( $R = 1$ ) fails and find spurious sources, the MMV case ( $R = 10$ ) localize the delay-Doppler pairs correctly. This in turn shows that using more antenna arrays improves the recovery performance for a fixed and weak time-frequency minimum separation. In the second experiment, we check a case where the sources are closer to each other as shown in top and bottom images of Figures 2. Again, we can see the superiority of using MMV ( $R = 30$ ) over SMV. All in all, one can infer from Figures 1 and 2 that under a fixed number of measurements  $N = 4$ , benefiting more MMVs can make the required minimum separation condition weaker (alternatively leading to a more relaxed condition). In the third experiment, we examine the noisy case where we consider complex noise  $\mathbf{W}$  with i.i.d. Gaussian elements such that the signal to noise ratio (SNR) defined as  $\text{SNR} = \frac{\|\mathbf{Y}\|_F^2}{\|\mathbf{W}\|_F^2}$  is equal to 10 dB. We choose two delay-Doppler pairs  $\mathbf{r}_1 = (0.2, 0.5)$  and  $\mathbf{r}_2 = (0.8, 0.5)$  and implement (25) with  $\eta = 0.8$ . As shown in top and bottom images of Figure 3, increasing the array elements (from  $R = 1$  in the top image to  $R = 50$  in the bottom image) can improve the recovery performance of delay-Doppler pairs.

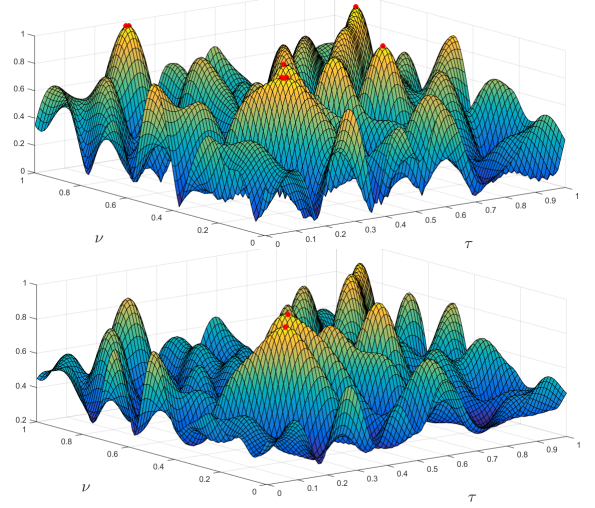


Fig. 3: Noisy case. The true sources are located at  $\mathbf{r}_1 = (0.2, 0.2)$ ,  $\mathbf{r}_2 = (0.3, 0.3)$ . We set  $N = 4$ ,  $\eta = 0.8$ ,  $\text{SNR} = 10\text{dB}$  and solve (25). Top and bottom images show  $\|\mathbf{q}(\mathbf{r})\|_2$  for SMV ( $R = 1$ ) and MMV ( $R = 50$ ) cases, respectively. Red markers show where  $\|\mathbf{q}(\mathbf{r})\|_2$  equals one.

#### APPENDIX A EQUIVALENCE OF (1) AND (2)

By sampling at rate  $\frac{1}{B}$ , the equation (1) can be displayed as follows:

$$y_m(\frac{p}{B}) = \sum_{j=1}^s b_{jm} x(\frac{p}{B} - \bar{\tau}_j) e^{i2\pi \bar{\nu}_j \frac{p}{B}}, p = -N, \dots, N, \quad (28)$$

we know that (by applying the discrete Fourier transform (DFT) and inverse DFT (IDFT) to  $x$ ):

$$\begin{aligned} x(\frac{p}{B} - \frac{\tau_j TB}{B}) &= x(\frac{p}{B} - \frac{\tau_j L}{B}) = x[p - \tau_j L] \\ &= \frac{1}{L} \sum_{k=-N}^N \left( \sum_{l=-N}^N x[l] e^{-\frac{i2\pi kl}{L}} \right) e^{-\frac{i2\pi \tau_j Lk}{L}} e^{\frac{i2\pi kp}{L}}. \end{aligned} \quad (29)$$

Substituting (29) into (28) leads to

$$\begin{aligned}
y\left(\frac{p}{B}\right) &= \frac{1}{L} \sum_{j=1}^s b_{jm} \sum_{k=-N}^N \left( \sum_{l=-N}^N x[l] e^{-\frac{i2\pi kl}{L}} \right) e^{-\frac{i2\pi \tau_j Lk}{L}} \\
e^{\frac{i2\pi kp}{L}} e^{i2\pi \nu_j p} &= \sum_{j=1}^s b_{jm} \frac{1}{L} \sum_{k,l=-N}^N x[l] e^{\frac{i2\pi k(p-l)}{L}} \\
e^{i2\pi [p\nu_j - k\tau_j]} &= \sum_{j=1}^s b_{jm} e^{i2\pi p\nu_j} \frac{1}{L} \sum_{l=-N}^N \sum_{k=-N}^N x[l] \\
e^{i2\pi [\frac{p-l}{L} - \tau_j]k} &= \sum_{j=1}^s b_{jm} e^{i2\pi p\nu_j} \frac{1}{L} \sum_{n=p-N}^{p+N} \sum_{k=-N}^N x[p-n], \\
e^{i2\pi [\frac{n}{L} - \tau_j]k} & \quad p = -N, \dots, N, \quad m = 1, \dots, R. \quad (30)
\end{aligned}$$

By using the definition (3), the fact that

$$\sum_{k=-N}^N D_N\left(\frac{k}{L} - \nu_j\right) e^{\frac{i2\pi pk}{L}} = e^{i2\pi p\nu_j}, \quad (31)$$

and the periodicity property of  $x_l$ , (30) becomes

$$\begin{aligned}
y_m\left(\frac{p}{B}\right) &= \sum_{j=1}^s b_{jm} e^{i2\pi p\nu_j} \frac{1}{L} \sum_{l=-N}^N \sum_{k=-N}^N x[l-p] e^{i2\pi [\frac{l}{L} - \tau_j]k} \\
&= \sum_{j=1}^s b_{jm} e^{i2\pi p\nu_j} \sum_{l=-N}^N x[l-p] D_N\left(\frac{l}{L} - \tau_j\right) \\
&= \sum_{j=1}^s b_{jm} \sum_{k=-N}^N D_N\left(\frac{k}{L} - \nu_j\right) e^{\frac{i2\pi pk}{L}} \sum_{l=-N}^N x[l-p] \\
&\quad \cdot D_N\left(\frac{l}{L} - \tau_j\right) = \\
&= \sum_{j=1}^s b_{jm} \sum_{k,l=-N}^N D_N\left(\frac{k}{L} - \nu_j\right) D_N\left(\frac{l}{L} - \tau_j\right) x_{l-p} e^{\frac{i2\pi pk}{L}}. \quad (32)
\end{aligned}$$

#### APPENDIX B PROOF OF PROPOSITION 1

We begin with  $\mathbf{\Lambda}$  which lies in the feasible set of (18), since due to (20) and the assumptions (17), we have:

$$\|\mathbf{G}^H \mathbf{\Lambda}\|_{\mathcal{A}}^d = \sup_{\mathbf{r} \in [0,1]^2} \|\mathbf{q}(\mathbf{r})\|_2 \leq 1. \quad (33)$$

We proceed by writing

$$\begin{aligned}
\|\mathbf{X}\|_{\mathcal{A}} &\geq \|\mathbf{G}^H \mathbf{\Lambda}\|_{\mathcal{A}}^d \|\mathbf{X}\|_{\mathcal{A}} \stackrel{(I)}{\geq} \text{Re} \langle \mathbf{G}^H \mathbf{\Lambda}, \mathbf{X} \rangle_F = \text{Re} \langle \mathbf{\Lambda}, \mathbf{Y} \rangle_F = \\
&\text{Re} \langle \mathbf{\Lambda}, \mathbf{G} \sum_{\mathbf{r}_j \in \mathcal{S}} c_j \mathbf{a}(\mathbf{r}_j) \hat{\boldsymbol{\varphi}}_j^H \rangle_F = \sum_{\mathbf{r}_j \in \mathcal{S}} \text{Re} c_j \langle \boldsymbol{\varphi}_j, \boldsymbol{\varphi}_j \rangle \stackrel{(II)}{=} \\
&\sum_{\mathbf{r}_j \in \mathcal{S}} c_j = \|\mathbf{X}\|_{\mathcal{A}}, \quad (34)
\end{aligned}$$

where the inequality (I) is due to (33), and the equality (II) stems from the assumptions in (17). The latter relation shows that all the inequalities must be turned into equality. Thus,  $\text{Re} \langle \mathbf{\Lambda}, \mathbf{Y} \rangle = \|\mathbf{X}\|_{\mathcal{A}}$  which in turn shows that  $(\mathbf{X}, \mathbf{\Lambda})$  are primal-dual optimal solutions. For uniqueness, we argue by contradiction and assume that there exists another optimal

primal solution  $\widehat{\mathbf{X}} = \sum_{\mathbf{r}_j \in \widehat{\mathcal{S}}} \widehat{c}_j \mathbf{a}(\mathbf{r}_j) \hat{\boldsymbol{\varphi}}_j^H$  where  $\widehat{\mathcal{S}} \neq \mathcal{S}$ . It holds that

$$\begin{aligned}
\|\widehat{\mathbf{X}}\|_{\mathcal{A}} &= \text{Re} \langle \mathbf{\Lambda}, \mathbf{G} \widehat{\mathbf{X}} \rangle = \text{Re} \langle \mathbf{\Lambda}, \mathbf{G} \sum_{\mathbf{r}_j \in \widehat{\mathcal{S}}} \widehat{c}_j \mathbf{a}(\mathbf{r}_j) \hat{\boldsymbol{\varphi}}_j^H \rangle = \\
&\sum_{\mathbf{r}_j \in \mathcal{S}} \text{Re} \widehat{c}_j \langle \hat{\boldsymbol{\varphi}}_j, \mathbf{q}(\mathbf{r}_j) \rangle + \sum_{\mathbf{r}_j \in \widehat{\mathcal{S}} \setminus \mathcal{S}} \text{Re} \widehat{c}_j \langle \hat{\boldsymbol{\varphi}}_j, \mathbf{q}(\mathbf{r}_j) \rangle < \sum_{\mathbf{r}_j \in \widehat{\mathcal{S}}} \widehat{c}_j \\
&= \|\widehat{\mathbf{X}}\|_{\mathcal{A}}, \quad (35)
\end{aligned}$$

where we used the assumptions in (17) in the last inequality. Hence, we have a contradiction and  $\widehat{\mathcal{S}} = \mathcal{S}$ . As a consequence, since  $\mathbf{a}(\mathbf{r}_j)$ ,  $\mathbf{r}_j \in \mathcal{S}$  are linearly independent, the optimal primal solution is unique.

#### APPENDIX C PROOF OF THEOREM 1

In this section, we prove Theorem 1 by constructing 2D vector-valued dual polynomial  $\mathbf{q}$  satisfying (17). Without loss of generality, we assume that  $N$  is even and define the squared Fejer kernel

$$K(t) := \frac{1}{M} \sum_{k=-N}^N g_k e^{i2\pi tk} := \left( \frac{\sin(M\pi t)}{M \sin(\pi t)} \right)^4, \quad M = \frac{N}{2} + 1, \quad (36)$$

where  $g_k$  is the discrete convolution of two triangular functions. First, in the following, we construct a deterministic dual polynomial satisfying (17) which is later used in our analysis:

$$\begin{aligned}
\bar{\mathbf{q}}(\mathbf{r}) &= \sum_{j=1}^s \bar{\alpha}_j \bar{G}(\mathbf{r} - \mathbf{r}_j) + \bar{\beta}_j \bar{G}^{(1,0)}(\mathbf{r} - \mathbf{r}_j) + \\
&\bar{\gamma}_j \bar{G}^{(0,1)}(\mathbf{r} - \mathbf{r}_j), \quad (37)
\end{aligned}$$

where the coefficients  $\bar{\alpha}_j, \bar{\beta}_j, \bar{\gamma}_j \in \mathbb{C}^{R \times 1}$ ,  $\bar{G}^{(m,n)} = \frac{\partial^m \partial^n \bar{G}}{\partial \tau^m \partial \nu^n}$  and  $\bar{G}(\mathbf{r}) := K(\tau)K(\nu)$ . An important requirement for the condition (17) to hold, is that  $\bar{\mathbf{q}}(\mathbf{r})$  reaches the local maxima by choosing the specific coefficients  $\bar{\alpha}_j, \bar{\beta}_j, \bar{\gamma}_j$  satisfying

$$\begin{aligned}
\bar{\mathbf{q}}(\mathbf{r}_j) &= \boldsymbol{\varphi}_j, & \forall \mathbf{r}_j \in \mathcal{S} \\
\bar{\mathbf{q}}^{(1,0)}(\mathbf{r}_j) &= \mathbf{0} \in \mathbb{C}^{R \times 1}, & \forall \mathbf{r}_j \in \mathcal{S} \\
\bar{\mathbf{q}}^{(0,1)}(\mathbf{r}_j) &= \mathbf{0} \in \mathbb{C}^{R \times 1}, & \forall \mathbf{r}_j \in \mathcal{S}, \quad (38)
\end{aligned}$$

where  $\bar{\mathbf{q}}^{(m,n)}(\mathbf{r}) := \frac{\partial^m \partial^n \bar{\mathbf{q}}}{\partial \tau^m \partial \nu^n}$ . Now, we construct the random polynomial  $\mathbf{q}(\mathbf{r})$  with function  $G_{(m,n)}(\mathbf{r}, \mathbf{r}_j)$ ,  $m, n = 0, 1$  as

$$\begin{aligned}
\mathbf{q}(\mathbf{r}) &= \sum_{j=1}^s \alpha_j G_{(0,0)}(\mathbf{r}, \mathbf{r}_j) + \beta_j G_{(1,0)}(\mathbf{r}, \mathbf{r}_j) \\
&+ \gamma_j G_{(0,1)}(\mathbf{r}, \mathbf{r}_j), \quad (39)
\end{aligned}$$

where the coefficients  $\alpha_k, \beta_k, \gamma_k$  are such that:

$$\begin{aligned}
\mathbf{q}(\mathbf{r}_j) &= \boldsymbol{\varphi}_j, & \forall \mathbf{r}_j \in \mathcal{S} \\
\mathbf{q}^{(1,0)}(\mathbf{r}_j) &= \mathbf{0} \in \mathbb{C}^{R \times 1}, & \forall \mathbf{r}_j \in \mathcal{S} \\
\mathbf{q}^{(0,1)}(\mathbf{r}_j) &= \mathbf{0} \in \mathbb{C}^{R \times 1}, & \forall \mathbf{r}_j \in \mathcal{S} \quad (40)
\end{aligned}$$

and  $\bar{G} := \mathbb{E}G$  is the expectation of kernel  $G$ . The dual polynomial  $\mathbf{q}$  in (39) can be regarded as a random version of  $\bar{\mathbf{q}}$  in (37) with the randomness introduced by  $\mathbf{x}$ .

### A. Choice of coefficients

We choose the coefficients  $\alpha_j, \beta_j, \gamma_j$  to construct  $\mathbf{q}(\mathbf{r})$  such that (40) holds with high probability. Writing (37) in matrix form, yields

$$\underbrace{\begin{bmatrix} \overline{D}^{(0,0)} & \kappa^{-1}\overline{D}^{(1,0)} & \kappa^{-1}\overline{D}^{(0,1)} \\ -\kappa^{-1}\overline{D}^{(1,0)} & -\kappa^{-2}\overline{D}^{(2,0)} & -\kappa^{-2}\overline{D}^{(1,1)} \\ -\kappa^{-1}\overline{D}^{(0,1)} & -\kappa^{-2}\overline{D}^{(1,1)} & -\kappa^{-2}\overline{D}^{(0,2)} \end{bmatrix}}_{\overline{D}} \begin{bmatrix} \overline{\alpha} \\ \kappa\overline{\beta} \\ \kappa\overline{\gamma} \end{bmatrix} = \begin{bmatrix} \overline{\Phi} \\ \mathbf{0} \\ \mathbf{0} \end{bmatrix}, \quad (41)$$

where  $(\kappa^2 = |K''(0)| = \sqrt{\frac{\pi^2}{3}(N^2 + 4N)}, K(0) = 1)$  and  $[\overline{D}^{(m,n)}]_{\kappa,j} := \overline{G}^{(m,n)}(\mathbf{r}_\kappa - \mathbf{r}_j)$ ,  $\overline{\Phi} = [\overline{\varphi}_1, \overline{\varphi}_2, \dots, \overline{\varphi}_s]^\top \in \mathbb{C}^{s \times R}$ ,  $\overline{\alpha} = [\overline{\alpha}_1, \overline{\alpha}_2, \dots, \overline{\alpha}_s]^\top \in \mathbb{C}^{s \times R}$ ,  $\overline{\beta} = [\overline{\beta}_1, \overline{\beta}_2, \dots, \overline{\beta}_s]^\top \in \mathbb{C}^{s \times R}$ ,  $\overline{\gamma} = [\overline{\gamma}_1, \overline{\gamma}_2, \dots, \overline{\gamma}_s]^\top \in \mathbb{C}^{s \times R}$  and  $\overline{D}$  is symmetric because  $\overline{D}^{(0,0)}$ ,  $\overline{D}^{(1,1)}$ ,  $\overline{D}^{(2,0)}$ ,  $\overline{D}^{(0,2)}$  are symmetric and  $\overline{D}^{(1,0)}$ ,  $\overline{D}^{(0,1)}$  are antisymmetric.  $\overline{D}$  is invertible and also the coefficients can be obtained as

$$\begin{bmatrix} \overline{\alpha} \\ \kappa\overline{\beta} \\ \kappa\overline{\gamma} \end{bmatrix} = \overline{D}^{-1} \begin{bmatrix} \overline{\Phi} \\ \mathbf{0} \\ \mathbf{0} \end{bmatrix} = \overline{\mathbf{L}}\Phi, \quad (42)$$

where  $\overline{\mathbf{L}} \in \mathbb{C}^{3s \times s}$  is the first  $s$  columns of  $\overline{D}^{-1}$ .

**Proposition 3.** [9, Proposition 8.2]  $\overline{D}$  is invertible and

$$\|\mathbf{I} - \overline{D}\| \leq 0.19808, \quad (43)$$

$$\|\overline{D}\| \leq 1.19808, \quad (44)$$

$$\|\overline{D}^{-1}\| \leq 1.24700. \quad (45)$$

Next, we choose the coefficients  $\alpha, \beta, \gamma \in \mathbb{C}^{s \times R}$  such that the conditions (40) hold. First, write (39) in matrix form as

$$\underbrace{\begin{bmatrix} D_{(0,0)}^{(0,0)} & \kappa^{-1}D_{(1,0)}^{(0,0)} & \kappa^{-1}D_{(0,1)}^{(0,0)} \\ -\kappa^{-1}D_{(0,0)}^{(1,0)} & -\kappa^{-2}D_{(1,0)}^{(1,0)} & -\kappa^{-2}D_{(0,1)}^{(1,0)} \\ -\kappa^{-1}D_{(0,0)}^{(0,1)} & -\kappa^{-2}D_{(1,0)}^{(0,1)} & -\kappa^{-2}D_{(0,1)}^{(0,1)} \end{bmatrix}}_{D} \begin{bmatrix} \alpha \\ \kappa\beta \\ \kappa\gamma \end{bmatrix} = \begin{bmatrix} \Phi \\ \mathbf{0} \\ \mathbf{0} \end{bmatrix}, \quad (46)$$

where  $[D_{(m',n')}^{(m,n)}]_{j,k} := G_{(m',n')}^{(m,n)}(\mathbf{r}_j, \mathbf{r}_k)$ ,  $\Phi = [\varphi_1, \varphi_2, \dots, \varphi_s]^\top \in \mathbb{C}^{s \times R}$ ,  $\alpha = [\alpha_1, \alpha_2, \dots, \alpha_s]^\top$ ,  $\beta = [\beta_1, \beta_2, \dots, \beta_s]^\top$ ,  $\gamma = [\gamma_1, \gamma_2, \dots, \gamma_s]^\top$ , where  $\alpha_j, \beta_j, \gamma_j \in \mathbb{C}^{R \times 1}$  with  $j = 1, \dots, s$ . To prove the existence of coefficients  $\alpha, \beta, \gamma$ , we show that  $D$  in (46) is invertible with high probability. Define the event

$$\zeta_\xi = \{\|D - \overline{D}\| \leq \xi\}. \quad (47)$$

If  $\zeta_\xi$  occurs with  $\xi \in (0, \frac{1}{4}]$ ,  $D$  is invertible since

$$\|\mathbf{I} - D\| \leq \|D - \overline{D}\| + \|\overline{D} - \mathbf{I}\| \leq \xi + 0.1908 \leq 0.4408. \quad (48)$$

Hence,  $\alpha_j, \beta_j, \gamma_j$  can be given as

$$\begin{bmatrix} \alpha \\ \kappa\beta \\ \kappa\gamma \end{bmatrix} = D^{-1} \begin{bmatrix} \Phi \\ \mathbf{0} \\ \mathbf{0} \end{bmatrix} = \mathbf{L}\Phi, \quad (49)$$

where  $\mathbf{L} \in \mathbb{C}^{3s \times s}$  is the first  $s$  columns of  $D^{-1}$ . To proceed, we use the following important lemma about the concentration of  $\mathbf{L}$  around  $\overline{\mathbf{L}}$ :

**Lemma 1.** ([9, Lemma 8.4]) If the event  $\zeta_\xi$  with  $\xi \in (0, \frac{1}{4}]$  occurs, then we have

$$\|\mathbf{L}\| \leq 2.5, \quad (50)$$

$$\|\mathbf{L} - \overline{\mathbf{L}}\| \leq 2.5\xi. \quad (51)$$

The following lemma provides conditions that  $\zeta_\xi$  occurs with high probability. We use this lemma to complete our proof.

**Lemma 2.** ([9, Lemma 8.6]) If

$$L \geq s \frac{c_3}{\xi^2} \log^2 \frac{18s^2}{\delta}, \quad (52)$$

then,

$$\mathbb{P}[\zeta_\xi] \geq 1 - \delta. \quad (53)$$

### B. Showing that $\mathbf{q}(\mathbf{r})$ and $\overline{\mathbf{q}}(\mathbf{r})$ are close on a grid

The goal of this section is to show that  $\mathbf{q}(\mathbf{r})$  and  $\overline{\mathbf{q}}(\mathbf{r})$  are close in a set of grid points  $\Omega$ .

**Lemma 3.** Let  $\Omega \subset [0, 1]^2$  be a finite set of points. Fix  $0 < \epsilon \leq 1$  and  $\delta > 0$ . If

$$L \geq \frac{s}{\epsilon^2} \max(c_2 \log^2(\frac{12s|\Omega|}{\delta}) \log(\frac{2(R+1)|\Omega|}{\delta}), c_3 \log(\frac{(R+1)|\Omega|}{\delta}) \log(\frac{18s^2}{\delta})), \quad (54)$$

then,  $\mathbb{P} \left[ \max_{\mathbf{r} \in \Omega} \frac{1}{\kappa^{m+n}} \|\mathbf{q}^{(m,n)}(\mathbf{r}) - \overline{\mathbf{q}}^{(m,n)}(\mathbf{r})\|_2 \leq \epsilon \right] \geq 1 - 4\delta$ .

It is straightforward to verify that  $(m, n)$ -th partial derivative of the dual polynomial  $\mathbf{q}(\mathbf{r})$  can be written as

$$\begin{aligned} \frac{1}{\kappa^{m+n}} \mathbf{q}^{(m,n)}(\mathbf{r}) &= \sum_{j=1}^s G_{(0,0)}^{(m,n)}(\mathbf{r}, \mathbf{r}_j) \alpha_j \\ &+ \frac{1}{\kappa} G_{(1,0)}^{(m,n)}(\mathbf{r}, \mathbf{r}_j) \kappa \beta_j + \frac{1}{\kappa} G_{(0,1)}^{(m,n)}(\mathbf{r}, \mathbf{r}_j) \kappa \gamma_j \\ &= (\mathbf{w}^{(m,n)}(\mathbf{r}))^H \mathbf{L}\Phi, \end{aligned} \quad (55)$$

where

$$\begin{aligned} (\mathbf{w}^{(m,n)}(\mathbf{r}))^H &:= \frac{1}{\kappa^{m+n}} [G_{(0,0)}^{(m,n)}(\mathbf{r}, \mathbf{r}_1), \dots, G_{(0,0)}^{(m,n)}(\mathbf{r}, \mathbf{r}_s), \\ &\frac{1}{\kappa} G_{(1,0)}^{(m,n)}(\mathbf{r}, \mathbf{r}_1), \dots, \frac{1}{\kappa} G_{(1,0)}^{(m,n)}(\mathbf{r}, \mathbf{r}_s), \\ &\frac{1}{\kappa} G_{(0,1)}^{(m,n)}(\mathbf{r}, \mathbf{r}_1), \dots, \frac{1}{\kappa} G_{(0,1)}^{(m,n)}(\mathbf{r}, \mathbf{r}_s)]. \end{aligned} \quad (56)$$

Due to  $\mathbb{E} [G_{(m',n')}^{(m,n)}(\mathbf{r}, \mathbf{r}_j)] = \overline{G}^{(m+m', n+n')}(\mathbf{r} - \mathbf{r}_j)$ , it holds that  $\mathbb{E} [\mathbf{w}^{(m,n)}(\mathbf{r})] = \overline{\mathbf{w}}^{(m,n)}(\mathbf{r})$ , where

$$\begin{aligned} (\overline{\mathbf{w}}^{(m,n)}(\mathbf{r}))^H &:= \frac{1}{\kappa^{m+n}} [\overline{G}^{(m,n)}(\mathbf{r} - \mathbf{r}_1), \dots, \overline{G}^{(m,n)}(\mathbf{r} - \mathbf{r}_s), \\ &\frac{1}{\kappa} \overline{G}^{(m+1,n)}(\mathbf{r} - \mathbf{r}_1), \dots, \frac{1}{\kappa} \overline{G}^{(m+1,n)}(\mathbf{r} - \mathbf{r}_s), \\ &\frac{1}{\kappa} \overline{G}^{(m,n+1)}(\mathbf{r} - \mathbf{r}_1), \dots, \frac{1}{\kappa} \overline{G}^{(m,n+1)}(\mathbf{r} - \mathbf{r}_s)]. \end{aligned} \quad (57)$$

Now, we can decompose (55) as follows

$$\begin{aligned} \frac{1}{\kappa^{m+n}} \mathbf{q}^{(m,n)}(\mathbf{r}) &= (\mathbf{w}^{(m,n)})^H(\mathbf{r}) \mathbf{L} \Phi = (\bar{\mathbf{w}}^{(m,n)})^H(\mathbf{r}) \bar{\mathbf{L}} \Phi \\ &\quad - \underbrace{(\mathbf{w}^{(m,n)}(\mathbf{r}) - \bar{\mathbf{w}}^{(m,n)})^H \mathbf{L} \Phi}_{\mathbf{I}_1^{(m,n)}(\mathbf{r})} + \underbrace{(\bar{\mathbf{w}}^{(m,n)})^H (\mathbf{L} - \bar{\mathbf{L}}) \Phi}_{\mathbf{I}_2^{(m,n)}(\mathbf{r})} \\ &= \frac{1}{\kappa^{m+n}} \bar{\mathbf{q}}^{(m,n)}(\mathbf{r}) + \mathbf{I}_1^{(m,n)}(\mathbf{r}) + \mathbf{I}_2^{(m,n)}(\mathbf{r}). \end{aligned} \quad (58)$$

The following lemmas show that  $\mathbf{I}_1^{(m,n)}(\mathbf{r})$  and  $\mathbf{I}_2^{(m,n)}(\mathbf{r})$  are small on a set of grid points  $\Omega$  with high probability.

**Lemma 4.** Consider  $\Omega \subset [0, 1]^2$  as a finite set of points and assume that  $m + n \leq 2$ . Then, we have

$$\mathbb{P} \left[ \max_{\mathbf{r} \in \Omega} \|\mathbf{I}_1^{(m,n)}(\mathbf{r})\|_2 \geq \epsilon \right] \leq \delta + \mathbb{P} \left[ \bar{\zeta}_{1/4} \right], \quad \forall \delta, \epsilon > 0 \quad (59)$$

provided  $L \geq \frac{c_2}{\epsilon^2} s \log^2 \left( \frac{12s|\Omega|}{\delta} \right) \log \left( \frac{2(R+1)|\Omega|}{\delta} \right)$ .

Proof. See Appendix D.

**Lemma 5.** Let  $\Omega \subset [0, 1]^2$  be a finite set of grid points and  $m + n \leq 2$ . For all  $\xi, \epsilon, \delta > 0$ , with  $\xi \leq \frac{\epsilon}{c_3 \sqrt{\log((R+1) \frac{|\Omega|}{\delta})}}$ ,

where  $c_3 \leq \frac{1}{4}$ , it holds that  $\mathbb{P} \left[ \max_{\mathbf{r} \in \Omega} \|\mathbf{I}_2^{(m,n)}(\mathbf{r})\|_2 \geq \epsilon |\zeta_\xi| \right] \leq \delta$ .

Proof. See Appendix E.

Now we can complete the proof of Lemma 3 by writing

$$\begin{aligned} \mathbb{P} \left[ \max_{\mathbf{r} \in \Omega} \frac{1}{\kappa^{m+n}} \|\mathbf{q}^{(m,n)}(\mathbf{r}) - \bar{\mathbf{q}}^{(m,n)}(\mathbf{r})\|_2 \geq 2\epsilon \right] \\ &= \mathbb{P} \left[ \max_{\mathbf{r} \in \Omega} \frac{1}{\kappa^{m+n}} \|\mathbf{I}_1^{(m,n)}(\mathbf{r}) + \mathbf{I}_2^{(m,n)}(\mathbf{r})\|_2 \geq 2\epsilon \right] \\ &\leq \mathbb{P} \left[ \max_{\mathbf{r} \in \Omega} \frac{1}{\kappa^{m+n}} \|\mathbf{I}_1^{(m,n)}(\mathbf{r})\|_2 \geq \epsilon \right] + \mathbb{P} \left[ \bar{\zeta}_\xi \right] \\ &\quad + \mathbb{P} \left[ \max_{\mathbf{r} \in \Omega} \frac{1}{\kappa^{m+n}} \|\mathbf{I}_2^{(m,n)}(\mathbf{r})\|_2 \geq \epsilon |\zeta_\xi| \right] \leq 4\delta, \end{aligned} \quad (60)$$

where we used the union bound and Lemmas 5, 4. By choosing  $\xi = \epsilon c_3 \log^{-\frac{1}{2}} \left( (R+1) \frac{|\Omega|}{\delta} \right)$ , the condition in Lemma 2 becomes  $L \geq s \left( \frac{c_1}{\epsilon c_3} \right) \log(2(R+1)) \log \left( \frac{18s^2}{\delta} \right)$  where  $c := \frac{c_1}{c_3}$ .

**C. Showing that  $\mathbf{q}(\mathbf{r})$  and  $\bar{\mathbf{q}}(\mathbf{r})$  are close for all  $\mathbf{r}$**

In this part, benefiting Lemma 3, we want to show that  $\mathbf{q}^{(m,n)}(\mathbf{r})$  is close to  $\bar{\mathbf{q}}^{(m,n)}(\mathbf{r})$  for all  $\mathbf{r} \in [0, 1]^2$  with high probability which is given in the following lemma.

**Lemma 6.** Let  $\epsilon, \delta > 0$ . It holds that

$$\max_{\mathbf{r} \in [0, 1]^2, (m,n): m+n \leq 2} \frac{1}{\kappa^{m+n}} \|\mathbf{q}^{(m,n)}(\mathbf{r}) - \bar{\mathbf{q}}^{(m,n)}(\mathbf{r})\|_2 \leq \epsilon \quad (61)$$

with probability at least  $1 - \delta$  provided that

$$L \geq \frac{sc}{\epsilon^2} \log^3 \left( \frac{c'RL^6}{\delta \epsilon^2} \right). \quad (62)$$

To prove, we first choose a set of sufficiently fine points in  $\Omega$  such that

$$\max_{\mathbf{r} \in [0, 1]^2} \min_{\mathbf{r}_g \in \Omega} \|\mathbf{r} - \mathbf{r}_g\|_\infty \leq \frac{\epsilon}{3\tilde{c}L^2 R^2} \quad (63)$$

with cardinality

$$|\Omega| = \left( \frac{3\tilde{c}L^{\frac{5}{2}} R^{\frac{1}{2}}}{\epsilon} \right)^2 = \frac{c' L^5 R}{\epsilon^2}. \quad (64)$$

By using the union bound over all six pairs  $(m, n)$  obeying  $m + n \leq 2$  and following Lemma 3, we find that

$$\begin{aligned} \mathbb{P} \left\{ \underbrace{\max_{\mathbf{r}_g \in \Omega, m+n \leq 2} \frac{1}{\kappa^{m+n}} \|\mathbf{q}^{(m,n)}(\mathbf{r}_g) - \bar{\mathbf{q}}^{(m,n)}(\mathbf{r}_g)\|_2}_{\mathcal{E}_1} \leq \frac{\epsilon}{3} \right\} \\ \geq 1 - \frac{\delta}{2}. \end{aligned} \quad (65)$$

To prove that the same result holds for all  $\mathbf{r} \in [0, 1]^2$ , it is necessary to show that

$$\mathbb{P} \left\{ \underbrace{\max_{\mathbf{r} \in [0, 1]^2, m+n \leq 2} \frac{1}{\kappa^{m+n}} \|\mathbf{q}^{(m,n)}(\mathbf{r})\|_2}_{\mathcal{E}_2} \leq \frac{\tilde{c}}{2} L^{\frac{3}{2}} \right\} \geq 1 - \frac{\delta}{2}, \quad (66)$$

which is proved in Appendix E-A. We also have  $\mathbb{P}\{\mathcal{E}_1 \cap \mathcal{E}_2\} \geq 1 - \delta$ . Since the event  $\mathcal{E}_1 \cap \mathcal{E}_2$  implies the event (61) (see Appendix F for the reason), Lemma 6 is concluded.

**D. Showing that  $\|\mathbf{q}(\mathbf{r})\|_2 \leq 1$  for all  $\mathbf{r} \notin \mathcal{S}$**

We begin with defining the following sets:

$$\Omega_{\text{far}} := \forall \mathbf{r} \in [0, 1]^2 : \min_{\mathbf{r}_j \in \mathcal{S}} \|\mathbf{r} - \mathbf{r}_j\|_\infty \geq \frac{0.2447}{N} \quad (67)$$

$$\Omega_{\text{close}} := \forall \mathbf{r} \notin \mathcal{S}, \mathbf{r}_j \in \mathcal{S} : 0 \leq \|\mathbf{r} - \mathbf{r}_j\|_\infty \leq \frac{0.2447}{N}. \quad (68)$$

The former argument (67) implies that the points are far from  $\mathbf{r}_j$  while the latter (68) include points that are close to it. In order to show that  $\mathbf{q}(\mathbf{r})$  in (39) satisfies (17), it is enough to show that  $\|\mathbf{q}(\mathbf{r})\|_2 \leq 1$  for  $\forall \mathbf{r} \in \Omega_{\text{far}}$  and  $\forall \mathbf{r} \in \Omega_{\text{close}}$ . To proceed, suppose that  $L \geq \frac{sc}{\epsilon^2} \log^3 \left( \frac{c'RL^6}{\delta \epsilon^2} \right)$ .

**Lemma 7.**  $\|\mathbf{q}(\mathbf{r})\|_2 \leq 1, \forall \mathbf{r} \in \Omega_{\text{far}}$  with high probability.

To prove this, take  $\epsilon = 0.002$  in (61) to reach

$$\|\mathbf{q}^{(m,n)}(\mathbf{r}) - \bar{\mathbf{q}}^{(m,n)}(\mathbf{r})\|_2 \leq 0.002. \quad (69)$$

By the triangular inequality, we have

$$\begin{aligned} \|\mathbf{q}^{(m,n)}(\mathbf{r})\|_2 &\leq \|\mathbf{q}^{(m,n)}(\mathbf{r}) - \bar{\mathbf{q}}^{(m,n)}(\mathbf{r})\|_2 + \|\bar{\mathbf{q}}^{(m,n)}(\mathbf{r})\|_2 \\ &\leq 0.9978, \end{aligned} \quad (70)$$

which verifies that  $\|\mathbf{q}(\mathbf{r})\|_2 \leq 1$  for far  $\mathbf{r}$ . For near  $\mathbf{r}$ , we state the following lemma.

**Lemma 8.**  $\|\mathbf{q}(\mathbf{r})\|_2 \leq 1, \forall \mathbf{r} \in \Omega_{\text{close}}$  with high probability.

To prove this, assume without loss of generality that  $\mathbf{0} \in \mathcal{S}$  i.e.  $\|\mathbf{r}\|_\infty \leq \frac{0.2447}{N}$ . A sufficient condition for Lemma 8 to hold, is to show that the Hessian matrix of  $\|\mathbf{q}(\mathbf{r})\|_2^2$ , i.e.,

$$\frac{1}{\kappa^2} \mathbf{H} = \frac{1}{\kappa^2} \begin{bmatrix} \frac{\partial^2 \|\mathbf{q}(\mathbf{r})\|_2^2}{\partial \tau^2} & \frac{\partial^2 \|\mathbf{q}(\mathbf{r})\|_2^2}{\partial \tau \partial \nu} \\ \frac{\partial^2 \|\mathbf{q}(\mathbf{r})\|_2^2}{\partial \tau \partial \nu} & \frac{\partial^2 \|\mathbf{q}(\mathbf{r})\|_2^2}{\partial \nu^2} \end{bmatrix} \quad (71)$$



is negative definite for all near  $\mathbf{r}$ . For this to hold, we should have

$$\frac{1}{\kappa^2} \text{tr}(\mathbf{H}) = \frac{\partial^2}{\partial \tau^2} \frac{1}{\kappa^2} \|\mathbf{q}(\mathbf{r})\|_2^2 + \frac{\partial^2}{\partial \nu^2} \frac{1}{\kappa^2} \|\mathbf{q}(\mathbf{r})\|_2^2 < 0 \quad (72)$$

and

$$\begin{aligned} \frac{1}{\kappa^2} \det(\mathbf{H}) &= \left( \frac{\partial^2}{\partial \tau^2} \frac{1}{\kappa^2} \|\mathbf{q}(\mathbf{r})\|_2^2 \right) \left( \frac{\partial^2}{\partial \nu^2} \frac{1}{\kappa^2} \|\mathbf{q}(\mathbf{r})\|_2^2 \right) \\ &- \left( \frac{\partial^2}{\partial \tau \partial \nu} \frac{1}{\kappa^2} \|\mathbf{q}(\mathbf{r})\|_2^2 \right)^2 > 0. \end{aligned} \quad (73)$$

To find  $\|\mathbf{q}(\mathbf{r})\|_2$  and its derivatives, we need to borrow some bounds from [18, Section, C.2] which states that  $\forall \mathbf{r} \in \Omega_{\text{close}}$  and  $N \geq 512$ , we have

$$\begin{aligned} \overline{G}(\mathbf{r}) &\geq 0.8113, \quad |\overline{G}^{(1,0)}(\mathbf{r})| \leq 0.8113, \\ \overline{G}^{(2,0)}(\mathbf{r}) &\leq -2.097N^2, \quad |\overline{G}^{(1,1)}(\mathbf{r})| \leq 0.6531N, \\ |\overline{G}^{(2,1)}(\mathbf{r})| &\leq 2.669N^2, \quad |\overline{G}^{(3,0)}(\mathbf{r})| \leq 8.070N^3. \end{aligned} \quad (74)$$

Introduce

$$\overline{Z}^{(m',n')}(\mathbf{r}) := \sum_{\mathbf{r}_j \in \mathcal{S}_0} |\overline{G}^{(m',n')}(\mathbf{r} - \mathbf{r}_j)|. \quad (75)$$

Again, based on [18, Table C.1], it holds that

$$\begin{aligned} \overline{Z}^{(0,0)}(\mathbf{r}) &\leq 6.405 \times 10^{-2}, \quad \overline{Z}^{(1,0)}(\mathbf{r}) \leq 0.1047N, \\ \overline{Z}^{(2,0)}(\mathbf{r}) &\leq 0.4019N, \quad \overline{Z}^{(1,1)}(\mathbf{r}) \leq 0.1642N^2, \\ \overline{Z}^{(2,1)}(\mathbf{r}) &\leq 0.675N^2, \quad \overline{Z}^{(3,0)}(\mathbf{r}) \leq 1.574N^3, \end{aligned} \quad (76)$$

and we also have [18, Section C.1]

$$\begin{aligned} \|\overline{\alpha}_j\|_2 &\leq \alpha_{\max} = 1 + 5.577 \times 10^{-2} \\ \|\overline{\alpha}_j\|_2 &\geq \alpha_{\min} = 1 - 5.577 \times 10^{-2} \\ \|\overline{\beta}_j\|_2 &\leq \beta_{\max} = \frac{2.93}{N} \times 10^{-2} \\ \|\overline{\gamma}_j\|_2 &\leq \gamma_{\max} = \frac{2.93}{N} \times 10^{-2}. \end{aligned} \quad (77)$$

We use the aforementioned formulas to obtain the bounds

$$\begin{aligned} \|\overline{\mathbf{q}}(\mathbf{r})\|_2 &= \left\| \sum_{j=1}^s \overline{G}^{(0,0)}(\mathbf{r} - \mathbf{r}_j) \overline{\alpha}_j + \overline{G}^{(1,0)}(\mathbf{r} - \mathbf{r}_j) \overline{\beta}_j \right. \\ &+ \overline{G}^{(0,1)}(\mathbf{r} - \mathbf{r}_j) \overline{\gamma}_j \left. \right\|_2 \leq \alpha_{\max} \left( |\overline{G}^{(0,0)}(\mathbf{r})| + \overline{Z}^{(0,0)}(\mathbf{r}) \right) \\ &+ 2\beta_{\max} \left( |\overline{G}^{(1,0)}(\mathbf{r})| + \overline{Z}^{(1,0)}(\mathbf{r}) \right) \leq 1.295 + \frac{0.0475}{N}. \end{aligned} \quad (78)$$

For the derivatives of  $\mathbf{q}$ , we have:

$$\begin{aligned} \|\overline{\mathbf{q}}^{(1,0)}\|_2 &\leq \alpha_{\max} \left( |\overline{G}^{(1,0)}(\mathbf{r})| + \overline{Z}^{(1,0)}(\mathbf{r}) \right) \\ &+ \beta_{\max} \left( |\overline{G}^{(2,0)}(\mathbf{r})| + \overline{Z}^{(2,0)}(\mathbf{r}) \right) + \gamma_{\max} \left( |\overline{G}^{(1,1)}(\mathbf{r})| \right. \\ &+ \overline{Z}^{(1,1)}(\mathbf{r}) \left. \right) \leq 0.08874 + 0.2148N. \end{aligned} \quad (79)$$

Other derivatives can be obtained using similar steps as follows:

$$\begin{aligned} \|\overline{\mathbf{q}}^{(1,1)}\|_2 &\leq 0.846N + 0.213N^2, \\ \|\overline{\mathbf{q}}^{(2,0)}\|_2 &\leq 0.5025N + 3.8845N^2. \end{aligned} \quad (80)$$

Now, we proceed (72) by writing

$$\begin{aligned} \frac{\partial^2}{\partial \tau^2} \frac{1}{\kappa} \|\mathbf{q}(\mathbf{r})\|_2^2 &= \frac{\partial}{\partial \tau} \frac{1}{\kappa^2} \langle \mathbf{q}^{(1,0)}(\mathbf{r}), \mathbf{q}(\mathbf{r}) \rangle = 2 \left\| \frac{1}{\kappa} \mathbf{q}^{(1,0)}(\mathbf{r}) \right\|_2^2 \\ &+ \frac{2}{\kappa^2} \text{Re} \left[ \left( \mathbf{q}^{(2,0)}(\mathbf{r}) \right)^H \mathbf{q}(\mathbf{r}) \right], \end{aligned} \quad (81)$$

where the first term can be bounded as

$$\begin{aligned} \left\| \frac{1}{\kappa} \mathbf{q}^{(1,0)}(\mathbf{r}) \right\|_2^2 &\leq \left\| \frac{1}{\kappa} \left( \mathbf{q}^{(1,0)}(\mathbf{r}) - \overline{\mathbf{q}}^{(1,0)}(\mathbf{r}) \right) \right\|_2^2 \\ &+ \left\| \frac{1}{\kappa} \overline{\mathbf{q}}^{(1,0)}(\mathbf{r}) \right\|_2^2 \leq \epsilon^2 + 0.0141. \end{aligned} \quad (82)$$

The first inequality above comes from the triangular inequality while the last one is based on Lemma 6, 79 and the fact that  $\kappa^2 \geq \frac{\pi^2}{3} N^2$ . The second term in (81) can be bounded by:

$$\begin{aligned} \frac{1}{\kappa^2} \text{Re} \left[ \left( \mathbf{q}^{(2,0)}(\mathbf{r}) \right)^H \mathbf{q}(\mathbf{r}) \right] &= \text{Re} \left[ \frac{2}{\kappa^2} \left( \mathbf{q}^{(2,0)}(\mathbf{r}) \right. \right. \\ &- \overline{\mathbf{q}}^{(2,0)}(\mathbf{r}) + \overline{\mathbf{q}}^{(2,0)}(\mathbf{r}) \left. \right)^H (\mathbf{q}(\mathbf{r}) - \overline{\mathbf{q}}(\mathbf{r}) + \overline{\mathbf{q}}(\mathbf{r})) \left. \right] = \\ &\text{Re} \left[ \frac{1}{\kappa^2} \left( \mathbf{q}^{(2,0)}(\mathbf{r}) - \overline{\mathbf{q}}^{(2,0)}(\mathbf{r}) \right)^H (\mathbf{q}(\mathbf{r}) - \overline{\mathbf{q}}(\mathbf{r})) \right] \\ &+ \text{Re} \left[ \frac{1}{\kappa^2} \left( \overline{\mathbf{q}}^{(2,0)}(\mathbf{r}) \right)^H \overline{\mathbf{q}}(\mathbf{r}) \right] \\ &+ \text{Re} \left[ \frac{1}{\kappa^2} \left( \mathbf{q}^{(2,0)}(\mathbf{r}) - \overline{\mathbf{q}}^{(2,0)}(\mathbf{r}) \right)^H \overline{\mathbf{q}}(\mathbf{r}) \right] \\ &+ \text{Re} \left[ \frac{1}{\kappa^2} \left( \overline{\mathbf{q}}^{(2,0)}(\mathbf{r}) \right)^H (\mathbf{q}(\mathbf{r}) - \overline{\mathbf{q}}(\mathbf{r})) \right] \\ &\leq \epsilon^2 - 0.307 + 1.129\epsilon + 1.181\epsilon \\ &\leq \epsilon^2 + 2.31\epsilon - 0.307. \end{aligned} \quad (83)$$

Substituting (83) and (82) into (81), yields to

$$\frac{1}{\kappa^2} \text{tr}(\mathbf{H}) \leq 8\epsilon^2 + 9.24\epsilon - 1.1712. \quad (84)$$

It is straightforward to verify that the above term is negative by setting  $\epsilon \leq 0.1$ . Next, we prove (73). The second term in (73) can be written as

$$\begin{aligned} \frac{\partial}{\partial \tau \partial \nu} \frac{1}{\kappa} \|\mathbf{q}(\mathbf{r})\|_2^2 &= \frac{2}{\kappa^2} \langle \mathbf{q}^{(1,0)}(\mathbf{r}), \mathbf{q}^{(0,1)}(\mathbf{r}) \rangle \\ &+ \frac{2}{\kappa^2} \langle \mathbf{q}^{(1,1)}(\mathbf{r}), \mathbf{q}(\mathbf{r}) \rangle. \end{aligned} \quad (85)$$

The upper-bound of the first term in (73) is obtained by

$$\begin{aligned} \frac{1}{\kappa^2} \langle \mathbf{q}^{(1,0)}(\mathbf{r}), \mathbf{q}^{(0,1)}(\mathbf{r}) \rangle &= \text{Re} \left[ \frac{1}{\kappa^2} \left( \mathbf{q}^{(1,0)}(\mathbf{r}) - \overline{\mathbf{q}}^{(1,0)}(\mathbf{r}) \right)^H \right. \\ &\left( \mathbf{q}^{(0,1)}(\mathbf{r}) - \overline{\mathbf{q}}^{(0,1)}(\mathbf{r}) \right) \left. \right] + \text{Re} \left[ \frac{1}{\kappa^2} \left( \overline{\mathbf{q}}^{(1,0)}(\mathbf{r}) \right)^H \overline{\mathbf{q}}^{(0,1)}(\mathbf{r}) \right] \\ &+ \text{Re} \left[ \frac{1}{\kappa^2} \left( \mathbf{q}^{(1,0)}(\mathbf{r}) - \overline{\mathbf{q}}^{(1,0)}(\mathbf{r}) \right)^H \overline{\mathbf{q}}^{(0,1)}(\mathbf{r}) \right] \\ &+ \text{Re} \left[ \frac{1}{\kappa^2} \left( \overline{\mathbf{q}}^{(1,0)}(\mathbf{r}) \right)^H \left( \mathbf{q}^{(0,1)}(\mathbf{r}) - \overline{\mathbf{q}}^{(0,1)}(\mathbf{r}) \right) \right] \\ &\leq \epsilon^2 + 0.238\epsilon + 0.0736, \end{aligned} \quad (86)$$

where the last inequality follows from (61),(80) and the fact that  $\kappa^2 \geq \frac{\pi^2}{3} N^2$ . By using similar steps as in (86), we reach

$$\frac{1}{\kappa^2} \langle \mathbf{q}^{(1,1)}(\mathbf{r}), \mathbf{q}(\mathbf{r}) \rangle \leq \epsilon^2 + 0.195\epsilon + 0.0736. \quad (87)$$

Substituting (86) and (87) into (85) yields to

$$\frac{\partial^2}{\partial \tau \partial \nu} \frac{1}{\kappa} \|\mathbf{q}(\mathbf{r})\|_2^2 \leq 4\epsilon^2 + 2.865\epsilon + 0.175. \quad (88)$$

By using the bound obtained for (88) and (81) and setting  $\epsilon = 0.05$ , (73) is satisfied. Finally, based on Lemmas 7 and 8, we can show that  $\|\mathbf{q}(\mathbf{r})\|_2 \leq 1, \forall \mathbf{r} \in [0, 1]^2 \setminus \mathcal{S}$ .

APPENDIX D  
PROOF OF LEMMA 4

Set  $\epsilon = 2.5ab$  and  $\Delta \mathbf{w}^{(m,n)} := \mathbf{w}^{(m,n)}(\mathbf{r}) - \bar{\mathbf{w}}^{(m,n)}(\mathbf{r})$ . For all  $a, b \geq 0$  we have

$$\begin{aligned} \mathbb{P}[\max_{\mathbf{r} \in \Omega} \|\mathbf{I}_1^{(m,n)}(\mathbf{r})\|_2 \geq 2.5ab] &= \mathbb{P}\left[\max_{\mathbf{r} \in \Omega} \|(\Delta \mathbf{w}^{(m,n)})^H \mathbf{L} \Phi\|_2 \geq 2.5ab\right] \\ &\leq \mathbb{P}\left[\bigcup_{\mathbf{r} \in \Omega} \left\{ \|(\Delta \mathbf{w}^{(m,n)})^H \mathbf{L} \Phi\|_2 \geq \|\mathbf{L}^H (\Delta \mathbf{w}^{(m,n)})\|_2 b \right\} \cup \left\{ \|\mathbf{L}^H \Delta \mathbf{w}^{(m,n)}\|_2 \geq 2.5a \right\}\right] \\ &\leq \mathbb{P}[\|\mathbf{L}\| \geq 2.5] + \sum_{\mathbf{r} \in \Omega} \left( \mathbb{P}\left[\|(\Delta \mathbf{w}^{(m,n)})^H \mathbf{L} \Phi\|_2 \geq \|\mathbf{L}^H (\Delta \mathbf{w}^{(m,n)})\|_2 b\right] + \mathbb{P}\left[\|\Delta \mathbf{w}^{(m,n)}\|_2 \geq a\right] \right) \\ &\stackrel{(I)}{\leq} \mathbb{P}[\bar{\zeta}_{\frac{1}{4}}] + (R+1)|\Omega|e^{-\frac{b^2}{8}} + \mathbb{P}\left[\|\Delta \mathbf{w}^{(m,n)}\|_2 \geq a\right] \\ &\leq \mathbb{P}[\bar{\zeta}_{\frac{1}{4}}] + \frac{\delta}{2} + \mathbb{P}\left[\|\Delta \mathbf{w}^{(m,n)}\|_2 \geq a\right], \end{aligned} \quad (89)$$

where (I) comes from the Hoeffding's inequality given below.

**Lemma 9.** [11](Hoeffding's inequality for vectors) Consider the rows of  $\Phi \in \mathbb{C}^{s \times R}$  be i.i.d. on the complex hypersphere  $\mathbb{S}^{R-1}$  with zero mean. Then, for all  $\mathbf{L}^H \Delta \mathbf{w}^{(m,n)} \in \mathbb{C}^s$ ,  $\mathbf{L}^H \Delta \mathbf{w}^{(m,n)} \neq \mathbf{0}$  and  $b \geq 0$ ,

$$\mathbb{P}(\|(\Delta \mathbf{w}^{(m,n)})^H \mathbf{L} \Phi\|_2 \geq \|\mathbf{L}^H \Delta \mathbf{w}^{(m,n)}\|_2 b) \leq (R+1)e^{-\frac{b^2}{8}}.$$

By using  $(R+1)|\Omega|e^{-\frac{b^2}{8}} \leq \frac{\delta}{2}$ , we obtain  $b = \sqrt{8 \log 2(R+1) \frac{|\Omega|}{\delta}}$ .

By using [9, Section 8.3.1] and choosing  $\mathbb{P}[\|\Delta \mathbf{w}^{(m,n)}\|_2 \geq a] \leq \frac{\delta}{2}$  and  $a = \sqrt{\frac{3s}{L}} 12^{\frac{3}{2}} c_1(\frac{c_2^2}{c})$ , we proceed (89) as follows:

$$\begin{aligned} \mathbb{P}\left[\max_{\mathbf{r} \in \Omega} \|\mathbf{I}_1^{(m,n)}(\mathbf{r})\|_2 \geq 360c_1\left(\frac{c_2^2}{\sqrt{c}}\right)\sqrt{\frac{s}{L}}\right] \\ \log\left(\frac{12s|\Omega|}{\delta}\right)\sqrt{\log\left(\frac{2(R+1)|\Omega|}{\delta}\right)} \leq \delta + \mathbb{P}(\bar{\zeta}_{\frac{1}{4}}) = 2\delta \end{aligned} \quad (90)$$

APPENDIX E  
PROOF OF LEMMA 5:

By the union bound:

$$\begin{aligned} \mathbb{P}\left[\max_{\mathbf{r} \in \Omega} \|\mathbf{I}_2^{(m,n)}(\mathbf{r})\|_2 \geq \epsilon \mid \zeta_\xi\right] \\ \leq \sum_{\mathbf{r} \in \Omega} \mathbb{P}\left[\|(\bar{\mathbf{w}}^{(m,n)}(\mathbf{r}))^H (\mathbf{L} - \bar{\mathbf{L}}) \Phi\|_2 \geq \epsilon \mid \zeta_\xi\right] \\ \leq \sum_{\mathbf{r} \in \Omega} \mathbb{P}\left[\|(\bar{\mathbf{w}}^{(m,n)}(\mathbf{r}))^H (\mathbf{L} - \bar{\mathbf{L}}) \Phi\|_2 \geq \|(\mathbf{L} - \bar{\mathbf{L}})^H \bar{\mathbf{w}}^{(m,n)}(\mathbf{r})\|_2 \frac{\epsilon}{(c_2 \xi)}\right] \\ \leq |\Omega|(R+1)e^{-\frac{(\frac{\epsilon}{(c_2 \xi)})^2}{8}} \leq \delta. \end{aligned} \quad (91)$$

A. Proof of (66)

We first find an upper-bound for  $\|\mathbf{q}^{(m,n)}(\mathbf{r})\|_2$  as follows:

$$\begin{aligned} \frac{1}{\kappa^{m+n}} \|\mathbf{q}^{(m,n)}(\mathbf{r})\|_2 &= \|(\mathbf{w}^{(m,n)})^H \mathbf{L} \Phi\|_2 \leq \|\mathbf{L}\| \|\Phi\| \|\mathbf{w}^{(m,n)}\|_2 \\ &\leq \|\mathbf{L}\| \|\Phi\|_F \|\mathbf{w}^{(m,n)}\|_2 \leq \|\mathbf{L}\| \sqrt{s} \sqrt{3s} \|\mathbf{w}^{(m,n)}\|_\infty \\ &\leq \|\mathbf{L}\| s \sqrt{3} \max_{j, (m', n') \in \{(0,0), (1,0), (0,1)\}} \frac{|G_{(m', n')}^{(m, n)}(\mathbf{r}, \mathbf{r}_j)|}{\kappa^{m+m'+n'+n}}, \end{aligned} \quad (92)$$

where we used the fact that  $\|\Phi\| \leq \|\Phi\|_F$  and for all  $\mathbf{r}$  and all  $\mathbf{r}_j$  we have [9, Equation 8.66]:

$$\frac{|G_{(m', n')}^{(m, n)}(\mathbf{r}, \mathbf{r}_j)|}{\kappa^{m+m'+n'+n}} \leq c_1 12^{\frac{3}{2}} \sqrt{L} \|\mathbf{x}\|_2^2. \quad (93)$$

By replacing (93) into (92) and using  $s \leq L$ , we have  $\frac{\|\mathbf{q}^{(m,n)}(\mathbf{r})\|_2}{\kappa^{m+n}} \leq 72c_1 L^{\frac{3}{2}} \|\mathbf{L}\| \|\mathbf{x}\|_2^2$ . Thus, by taking  $\frac{\tilde{c}}{2} = (2.5) \cdot (3) \cdot (72)c_1$ ,

$$\begin{aligned} \mathbb{P}\left[\max_{\mathbf{r} \in [0,1]^2, m+n \leq 2} \|\mathbf{q}^{(m,n)}(\mathbf{r})\|_2 \geq \frac{\tilde{c}}{2} L^{\frac{3}{2}}\right] \\ \leq \mathbb{P}[\|\mathbf{L}\| \|\mathbf{x}\|_2^2 \geq (2.5) \cdot (3)] \\ \leq \mathbb{P}[\|\mathbf{L}\| \geq 2.5] + \mathbb{P}[\|\mathbf{x}\|_2^2 \geq 3] \leq \frac{\delta}{2}, \end{aligned} \quad (94)$$

where we used the fact that  $\mathbb{P}[\|\mathbf{x}\|_2^2 \geq 3] \leq \frac{\delta}{4}$  [9, Equation 8.69]. The last inequality follows from  $\mathbb{P}[\|\mathbf{L}\| \geq 2.5] \leq \mathbb{P}[\bar{\zeta}_{\frac{1}{4}}] \leq \frac{\delta}{4}$  (from Lemma 1).

APPENDIX F  
THE REASON THAT  $\mathcal{E}_1, \mathcal{E}_2$  IMPLY (61)

Let  $\mathbf{r}_g$  be the closest points in  $\Omega$  to  $\mathbf{r}$  with respect to  $\ell_\infty$ -measure. By the triangle inequality:

$$\begin{aligned} \frac{1}{\kappa^{m+n}} \|\mathbf{q}^{(m,n)}(\mathbf{r}) - \bar{\mathbf{q}}^{(m,n)}(\mathbf{r})\|_2 \\ \leq \frac{1}{\kappa^{m+n}} \left[ \|\mathbf{q}^{(m,n)}(\mathbf{r}) - \mathbf{q}^{(m,n)}(\mathbf{r}_g)\|_2 \right. \\ \left. + \|\mathbf{q}^{(m,n)}(\mathbf{r}_g) - \bar{\mathbf{q}}^{(m,n)}(\mathbf{r}_g)\|_2 \right. \\ \left. + \|\bar{\mathbf{q}}^{(m,n)}(\mathbf{r}_g) - \bar{\mathbf{q}}^{(m,n)}(\mathbf{r})\|_2 \right]. \end{aligned} \quad (95)$$

Next, we obtain upper-bounds for the composing terms of the above relation, separately. For the first term, we have:

$$\begin{aligned} \|\mathbf{q}^{(m,n)}(\mathbf{r}) - \mathbf{q}^{(m,n)}(\mathbf{r}_g)\|_2 &\leq \sqrt{R} \max_i |\mathbf{q}^{(m,n)}(\mathbf{r}) - \mathbf{q}^{(m,n)}(\mathbf{r}_g)|_i. \end{aligned} \quad (96)$$

We proceed (96) by writing

$$\begin{aligned} |\mathbf{q}^{(m,n)}(\mathbf{r}) - \mathbf{q}^{(m,n)}(\mathbf{r}_g)|_i &= |\mathbf{q}^{(m,n)}(\tau, \nu) - \mathbf{q}^{(m,n)}(\tau, \nu_g)| \\ &+ |\mathbf{q}^{(m,n)}(\tau, \nu_g) - \mathbf{q}^{(m,n)}(\tau_g, \nu_g)|_i \\ &\leq |\mathbf{q}^{(m,n)}(\tau, \nu) - \mathbf{q}^{(m,n)}(\tau, \nu_g)|_i \\ &+ |\mathbf{q}^{(m,n)}(\tau, \nu_g) - \mathbf{q}^{(m,n)}(\tau_g, \nu_g)|_i \\ &\leq |\nu - \nu_g| \sup_z |\mathbf{q}^{(m,n+1)}(\tau, z)|_i \\ &+ |\tau - \tau_g| \sup_z |\mathbf{q}^{(m+1,n)}(z, \nu_g)|_i \\ &\leq |\nu - \nu_g| 2\pi N \sup_z \|\mathbf{q}^{(m,n)}(\tau, z)\|_2 \\ &+ |\tau - \tau_g| 2\pi N \sup_z \|\mathbf{q}^{(m,n)}(z, \tau)\|_2, \end{aligned} \quad (97)$$

where in the last step, we used Bernstein's polynomial inequality [27, Corollary 8]. Substituting (66) into (97), we reach

$$\begin{aligned} & \frac{1}{\kappa^{m+n}} \|\mathbf{q}^{(m,n)}(\mathbf{r}) - \mathbf{q}^{(m,n)}(\mathbf{r}_g)\|_2 \\ & \leq \frac{\tilde{c}}{2} L^{\frac{5}{2}} R^{\frac{1}{2}} (|\tau - \tau_g| + |\nu - \nu_g|) \\ & \leq \tilde{c} L^{\frac{5}{2}} R^{\frac{1}{2}} \|\mathbf{r} - \mathbf{r}_g\|_\infty \leq \frac{\epsilon}{3}. \end{aligned} \quad (98)$$

Similarly, we have

$$\frac{1}{\kappa^{m+n}} \|\bar{\mathbf{q}}^{(m,n)}(\mathbf{r}_g) - \bar{\mathbf{q}}^{(m,n)}(\mathbf{r})\|_2 \leq \frac{\epsilon}{3}. \quad (99)$$

Substituting (65), (98), (99) into (95) leads to

$$\frac{1}{\kappa^{m+n}} \|\mathbf{q}^{(m,n)}(\mathbf{r}) - \bar{\mathbf{q}}^{(m,n)}(\mathbf{r})\|_2 \leq \epsilon \quad (100)$$

for all  $(m, n) : m + n \leq 2$  and for all  $\mathbf{r} \in [0, 1]^2$ .

## REFERENCES

- [1] R. Handbook, "by mi skolnik," 2008.
- [2] K. G. Puschmann and F. Kneer, "On super-resolution in astronomical imaging," *Astronomy & Astrophysics*, vol. 436, no. 1, pp. 373–378, 2005.
- [3] X. Luo and G. B. Giannakis, "Low-complexity blind synchronization and demodulation for (ultra-) wideband multi-user ad hoc access," *IEEE Transactions on Wireless communications*, vol. 5, no. 7, pp. 1930–1941, 2006.
- [4] V. Khaidukov, E. Landa, and T. J. Moser, "Diffraction imaging by focusing-defocusing: An outlook on seismic superresolution," *Geophysics*, vol. 69, no. 6, pp. 1478–1490, 2004.
- [5] C. W. McCutchen, "Superresolution in microscopy and the abbe resolution limit," *JOSA*, vol. 57, no. 10, pp. 1190–1192, 1967.
- [6] A. H. Sayed, A. Tarighat, and N. Khajehnouri, "Network-based wireless location: challenges faced in developing techniques for accurate wireless location information," *IEEE signal processing magazine*, vol. 22, no. 4, pp. 24–40, 2005.
- [7] P. Stoica, R. L. Moses, *et al.*, "Spectral analysis of signals," 2005.
- [8] A. Jakobsson, A. L. Swindlehurst, and P. Stoica, "Subspace-based estimation of time delays and doppler shifts," *IEEE Transactions on Signal Processing*, vol. 46, no. 9, pp. 2472–2483, 1998.
- [9] R. Heckel, V. I. Morgenshtern, and M. Soltanolkotabi, "Super-resolution radar," *Information and Inference: A Journal of the IMA*, vol. 5, no. 1, pp. 22–75, 2016.
- [10] Y. Li and Y. Chi, "Off-the-grid line spectrum denoising and estimation with multiple measurement vectors," *IEEE Transactions on Signal Processing*, vol. 64, no. 5, pp. 1257–1269, 2015.
- [11] Z. Yang and L. Xie, "Exact joint sparse frequency recovery via optimization methods," *IEEE Transactions on Signal Processing*, vol. 64, no. 19, pp. 5145–5157, 2016.
- [12] E. J. Candès, J. Romberg, and T. Tao, "Robust uncertainty principles: Exact signal reconstruction from highly incomplete frequency information," *IEEE Transactions on information theory*, vol. 52, no. 2, pp. 489–509, 2006.
- [13] S. Daei, F. Haddadi, and A. Amini, "Exploiting prior information in block-sparse signals," *IEEE Transactions on Signal Processing*, vol. 67, no. 19, pp. 5093–5102, 2019.
- [14] S. Daei, F. Haddadi, and A. Amini, "Distribution-aware block-sparse recovery via convex optimization," *IEEE Signal Processing Letters*, vol. 26, no. 4, pp. 528–532, 2019.
- [15] V. Chandrasekaran, B. Recht, P. A. Parrilo, and A. S. Willsky, "The convex geometry of linear inverse problems," *Foundations of Computational mathematics*, vol. 12, no. 6, pp. 805–849, 2012.
- [16] R. O. Schmidt, "A signal subspace approach to multiple emitter location and spectral estimation," 1982.
- [17] B. Ottersten, M. Viberg, and T. Kailath, "Performance analysis of the total least squares esprit algorithm," *IEEE Transactions on Signal Processing*, vol. 39, no. 5, pp. 1122–1135, 1991.
- [18] E. J. Candès and C. Fernandez-Granda, "Towards a mathematical theory of super-resolution," *Communications on pure and applied Mathematics*, vol. 67, no. 6, pp. 906–956, 2014.
- [19] G. Tang, B. N. Bhaskar, P. Shah, and B. Recht, "Compressed sensing off the grid," *IEEE transactions on information theory*, vol. 59, no. 11, pp. 7465–7490, 2013.
- [20] R. Heckel, "Super-resolution mimo radar," in *2016 IEEE International Symposium on Information Theory (ISIT)*, pp. 1416–1420, IEEE, 2016.
- [21] D. Slepian, "On bandwidth," *Proceedings of the IEEE*, vol. 64, no. 3, pp. 292–300, 1976.
- [22] G. Durisi, V. I. Morgenshtern, and H. Bolcskei, "On the sensitivity of continuous-time noncoherent fading channel capacity," *IEEE Transactions on Information Theory*, vol. 58, no. 10, pp. 6372–6391, 2012.
- [23] D. Bertsekas and A. Nedic, "Convex analysis and optimization (conservative)," 2003.
- [24] C. Fernandez-Granda, "Super-resolution of point sources via convex programming," *Information and Inference: A Journal of the IMA*, vol. 5, no. 3, pp. 251–303, 2016.
- [25] B. Dumitrescu, *Positive Trigonometric Polynomials and Signal Processing Applications*. Springer, 2017.
- [26] M. Grant and S. Boyd, "Cvx: Matlab software for disciplined convex programming, version 2.1," 2014.
- [27] L. A. Harris, "Bernstein's polynomial inequalities and functional analysis," *Irish Mathematics Society Bull.*, p. 18, 1996.